tavidin, biotinylated alkaline phosphatase, and a chemiluminescent substrate system (Phototope-Star Detection kit; New England BioLabs, Beverly, MA, USA). We counted distinct bands as corresponding to clonal T-cell expansions. Although bands usually were easily recognized visually, a densitometer (ACD-25DX; ATTO Technology, Tokyo, Japan) was also used to confirm the presence of the bands. If one or more distinct bands were present in a certain Vβ gene family, the existence of clonally expanded T-cells was demonstrated. The presence of clonally expanded T-cells in each TCR Vβ gene family was individually assessed, and then the proportion of patients (or healthy volunteers) with clonally expanded T-cells was calculated for each TCR Vβ gene.

2.3. DNA Sequencing

TCR Vβ gene transcripts obtained before and after eradication therapy from one patient who had recovered from thrombocytopenia after *H pylori* eradication were extracted from the SSCP gel and cloned with a TA cloning kit (Invitrogen, Carlsbad, CA, USA). Approximately 20 plaques were randomly chosen and subjected to dideoxy direct sequencing.

2.4. Statistical Analysis

Differences in proportions among the groups were evaluated by the Kruskal-Wallis test, the Student *t* test, or the chi-square test. A *P* value <.05 was considered statistically significant.

3. Results

3.1. Analysis of the Clonally Expanded T-Cells in ITP Patients with H pylori Infection

We performed SSCP analyses of 20 major TCR Vβ gene families in patients with *H pylori* infection to investigate whether clonally expanded T-cells were present in PB. The median number of TCR Vβ gene families with clonally expanded T-cells in responders, nonresponders, and healthy subjects was 7 (range, 1-21), 3.5 (range, 2-11), and 4 (range, 1-6), respectively. The number of Vβ gene families with clonally expanded T-cells was significantly greater in responders (P = .032).

TCR Vβ subfamilies that frequently (>50% of cases) revealed clonally expanded T-cells were observed in 7 families (Vβ1, Vβ2, Vβ5.2, Vβ7, Vβ11, Vβ15, and Vβ19) in responders, 2 families (Vβ1 and Vβ5.1) in nonresponders, and 3 families (Vβ7, Vβ10, and Vβ11) in healthy volunteers (Figure 1). We analyzed the differences in Vβ usage of clonally expanded T-cells among responders, nonresponders, and healthy volunteers and found that the usage of Vβ5.2, Vβ15, and Vβ19 genes of clonally expanded T-cells was significantly higher in responders than in nonresponders or healthy volunteers (Vβ5.2, P = .023; Vβ15, P = .004; Vβ19, P = .036). We investigated whether the distinct bands in the SSCP analysis of Vβ5.2 (patients 1, 2, 3, and 6), Vβ15 (patients 3, 4, and 8), or Vβ19 (patients 3, 6, and 8) genes that were found in some responders before therapy disappeared after therapy. Disappearance of distinct bands from Vβ5.2, Vβ15, and Vβ19 genes was observed in none of 4 responders, 1 (patient 3) of 3 responders, and 1 (patient 3) of 3 responders, respectively (data not shown).

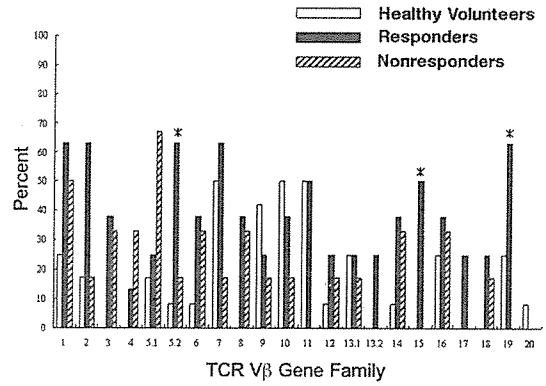

Figure 1. T-cell receptor (TCR) Vβ subfamily usage by clonally accumulated T-cells for responders, nonresponders, and healthy volunteers. Peripheral blood samples from patients with idiopathic thrombocytopenic purpura were obtained before eradication therapy and analyzed. If one or more distinct bands for a given Vβ gene were present in the single-strand conformation polymorphism analysis, the existence of clonally expanded T-cells was confirmed. The presence of clonally expanded T-cells for each TCR Vβ gene was individually assessed, and then the proportion of patients (or healthy volunteers) with clonal T-cell expansion was calculated for each TCR Vβ gene. Responders indicates patients who recovered from thrombocytopenia after successful *Helicobacter pylori* eradication; nonresponders, patients who failed to recover from thrombocytopenia even after *H pylori* was successfully eradicated. *Vβ5.2, Vβ15, and Vβ19 gene usage was significantly higher in responders than in nonresponders or healthy volunteers (P = .023, .004, and .036, respectively).

We compared nonresponders and healthy volunteers with respect to Vβ usage by clonally expanded T-cells and found Vβ3, Vβ4, Vβ5.1, and Vβ8 gene usage to be significantly higher in nonresponders (P = .034, .034, .034, and .034, respectively).

3.2. DNA Sequencing of TCR CDR3

In a patient (patient 1) who recovered from thrombocytopenia after *H pylori* eradication, the distinct band that was seen in the SSCP analysis of the Vβ8 gene before eradication therapy disappeared after eradication therapy (Figure 2). To confirm the disappearance of clonally expanded T-cells in Vβ8 following *H pylori* eradication, we determined the CDR3 DNA sequences of the TCR Vβ genes. In the sample obtained before *H pylori* eradication, all 18 subcloned genes showed the same sequence. However, in the sample obtained after *H pylori* eradication, all 19 subcloned genes showed different sequences, and none of these sequences were identical to the sequence seen before *H pylori* eradication (Table 2).

4. Discussion

We performed an SSCP analysis of TCR Vβ-chain genes of PB T-cells from ITP patients with *H pylori* infection and

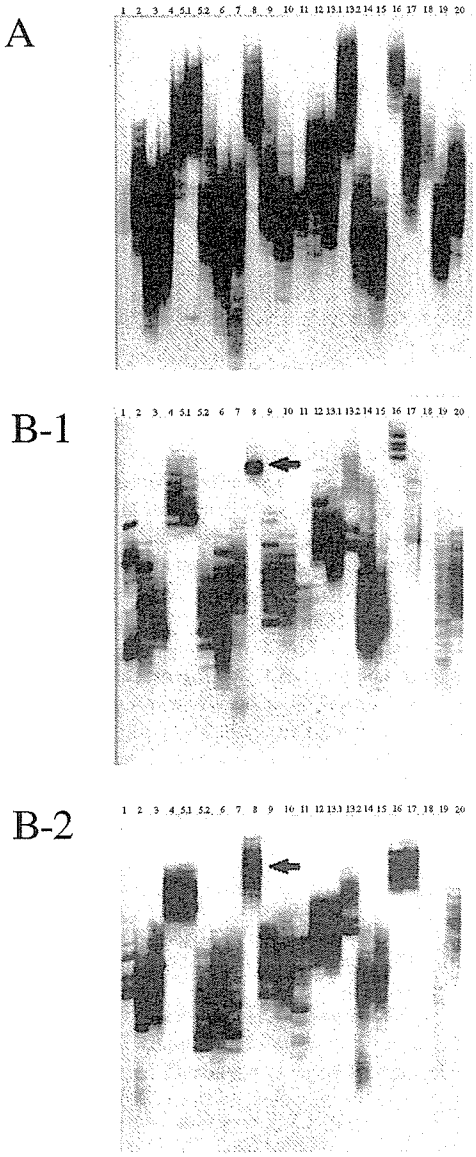

Figure 2. Single-strand conformation polymorphism analysis of T-cell receptor (TCR) Vβ genes in peripheral blood T-cells. The number at the top of each lane indicates the TCR Vβ gene subfamily. Results obtained from a typical healthy control subject (A) and patient 1 (responder) (B) are shown. In patient 1, a distinct band for the Vβ8 gene segment present before *Helicobacter pylori* eradication (B-1) disappeared after *H pylori* eradication (B-2) (arrows).

investigated T-cell repertoire usage by clonally expanded T-cells. The number of TCR Vβ gene families with clonally expanded T-cells was significantly higher in the patients with *H pylori* infection who subsequently recovered from thrombocytopenia after successful eradication therapy (responders) than in the patients who failed to recover from thrombocytopenia after successful eradication therapy (nonresponders). In addition, the usage of Vβ5.2, Vβ15, and

Table 2.
Deduced Amino Acid Sequences of the T-Cell Receptor (TCR) β Chains Carrying the Vβ Gene Segment Derived from the Peripheral Blood of Patient 1

Vβ8	nDn	Jβ (Gene Segment)	TCR β Chains, n
Before *Helicobacter pylori* eradication			
CASS	FSYCSA	NYGYT (J1S2)	18 (100%)
After *Helicobacter pylori* eradication			
CASSL	AWSGRY	TGELF (J2S2)	1 (5.3%)
CAS	RTTGG	SYEQY (J2S7)	1 (5.3%)
CASS	FSGGR	ETQYF (J2S5)	1 (5.3%)
CASS	KTGYE	QYFGP (J2S3)	1 (5.3%)
CAS	SRLAGGHPPT	QYFGP (J2S7)	1 (5.3%)
CAS	TRPEGGT	YNEQFF (J2S1)	1 (5.3%)
CAS	EEG	NTEAF (J1S1)	1 (5.3%)
CAS	SRFPAGA	YEQYF (J2S7)	1 (5.3%)
CA	SRPLAP	QETQYF (J2S5)	1 (5.3%)
CASS	SATV	SYEQY (J2S7)	1 (5.3%)
CASS	PRLDG	SYEQY (J2S7)	1 (5.3%)
CASS	RDFRA	NYGYT (J1S2)	1 (5.3%)
CASS	FGGTAR	QETQYF (J2S5)	1 (5.3%)
CASS	GTGTTSD	EQFFGPG (J2S1)	1 (5.3%)
CASSL	RPY	QPQHFG (J1S5)	1 (5.3%)
CAS	QGQH	NSPLHF (J1S6)	1 (5.3%)
CAS	NRLAGGHP	DTQYFGP (J2S3)	1 (5.3%)
CASSL	ELQDGYA	FGSGTRL (J1S2)	1 (5.3%)
CAS	RL	SGANVLT (J2S6)	1 (5.3%)

Vβ19 genes by clonally expanded T-cells was significantly higher in responders than in nonresponders. This difference notably does not derive from the presence or absence of *H pylori* infection, because all of the patients had been infected with *H pylori*. These results suggest that some clonally expanded T-cells with specific TCR Vβ subfamily usage are present in patients with *H pylori*–related ITP. Distinct bands seen in the SSCP analysis of Vβ genes before *H pylori* eradication therapy in some of the responders disappeared after *H pylori* eradication therapy. Furthermore, we confirmed the disappearance of clonally expanded T-cells after *H pylori* eradication therapy in a patient with *H pylori*–related ITP by analyzing the DNA sequences of CDR3 of Vβ genes. Our results indicate that clonally expanded T-cells were abrogated by *H pylori* eradication and suggest that the disappearance of clonally expanded T-cells was responsible for platelet recovery.

H pylori infection is associated with various autoimmune diseases, including rheumatoid arthritis, Sjögren syndrome, and autoimmune hypothyroidism [22-25]. Clinical data from patients with these disorders raise the possibility that immune reactions against *H pylori* have pivotal roles in the onset of autoimmune diseases. As for *H pylori*–related ITP, why *H pylori* eradication is able to induce platelet recovery is unknown. However, one possible explanation is that anti–*H pylori* antibodies bind to platelets in the presence of cross-mimicry between platelet surface antigens and *H pylori* antigens, resulting in platelet destruction. This speculation is supported by recent work demonstrating that platelet-associated immunoglobulin possesses cross-reactivity to

H pylori cytotoxin-associated gene A (CagA) [26]. If this mechanism operates in *H pylori*–related ITP, it strongly suggests that *H pylori* eradication induces a reduction in the T-cell clones against CagA that drive B-cells to produce cross-reactive antibodies, resulting in the reduction of cross-reactive antibodies. Our data demonstrating the subsequent disappearance of clonally expanded T-cells after *H pylori* eradication support this speculation.

Cytotoxic T-cell–mediated lysis of autologous platelets has recently been demonstrated in active ITP, and T-cell–mediated cytotoxicity has been suggested to be an alternative mechanism of platelet destruction in ITP [27]. Therefore, it is also possible that clonally expanded T-cells observed in *H pylori*–related ITP are cytotoxic T-cells against *H pylori* with cross-reactivity to platelets.

In conclusion, our findings suggest that specific T-cell clones accumulate in *H pylori*–related ITP and that these clones may be associated with immune-mediated platelet destruction. Further studies are needed to elucidate the role of the clonally expanded T-cells observed in *H pylori*–related ITP.

References

1. Gasbarrini A, Franceschi F, Tartaglione R, Landolfi R, Pola P, Gasbarrini G. Regression of autoimmune thrombocytopenia after eradication of *Helicobacter pylori*. *Lancet*. 1998;352:878.
2. Emilia G, Longo G, Luppi M, et al. *Helicobacter pylori* eradication can induce platelet recovery in idiopathic thrombocytopenic purpura. *Blood*. 2001;97:812-814.
3. Kohda K, Kuga T, Kogawa K, et al. Effect of *Helicobacter pylori* eradication on platelet recovery in Japanese patients with chronic idiopathic thrombocytopenic purpura and secondary autoimmune thrombocytopenic purpura. *Br J Haematol*. 2002;118:584-588.
4. Veneri D, Franchini M, Gottardi M, et al. Efficacy of *Helicobacter pylori* eradication in raising platelet count in adult patients with idiopathic thrombocytopenic purpura. *Haematologica*. 2002;87: 1177-1179.
5. Hino M, Yamane T, Park K, et al. Platelet recovery after eradication of *Helicobacter pylori* in patients with idiopathic thrombocytopenic purpura. *Ann Hematol*. 2003;82:30-32.
6. Hashino S, Mori A, Suzuki S, et al. Platelet recovery in patients with idiopathic thrombocytopenic purpura after eradication of *Helicobacter pylori*. *Int J Hematol*. 2003;77:188-191.
7. Ando T, Tsuzuki T, Mizuno T, et al. Characteristics of *Helicobacter pylori*-induced gastritis and the effect of *H. pylori* eradication in patients with chronic idiopathic thrombocytopenic purpura. *Helicobacter*. 2004;9:443-452.
8. Sato R, Murakami K, Watanabe K, et al. Effect of *Helicobacter pylori* eradication on platelet recovery in patients with chronic idiopathic thrombocytopenic purpura. *Arch Intern Med*. 2004;164: 1904-1907.
9. Fujimura K, Kuwana M, Kurata Y, et al. Is eradication therapy useful as the first line of treatment in *Helicobacter pylori*-positive idiopathic thrombocytopenic purpura? Analysis of 207 eradicated chronic ITP cases in Japan. *Int J Hematol*. 2005;81:162-168.
10. Inaba T, Mizuno M, Take S, et al. Eradication of *Helicobacter pylori* increases platelet count in patients with idiopathic thrombocytopenic purpura in Japan. *Eur J Clin Invest*. 2005;35:214-219.
11. Stasi R, Rossi Z, Stipa E, Amadori S, Newland AC, Provan D. *Helicobacter pylori* eradication in the management of patients with idiopathic thrombocytopenic purpura. *Am J Med*. 2005;118: 414-419.
12. Jarque I, Andrew R, Llopis I, et al. Absence of platelet response after eradication of *Helicobacter pylori* infection in patients with chronic idiopathic thrombocytopenic purpura. *Br J Haematol*. 2001;115:1002-1003.
13. Michel M, Khellaf M, Desforges L, et al. Autoimmune thrombocytopenic purpura and *Helicobacter pylori* infection. *Arch Intern Med*. 2002;162:1033-1036.
14. Michel M, Cooper N, Jean C, Frissora C, Bussel JB. Does *Helicobater pylori* initiate or perpetuate immune thrombocytopenic purpura? *Blood*. 2004;103:890-896.
15. Shimomura T, Fujimura K, Takafuta T, et al. Oligoclonal accumulation of T cells in peripheral blood from patients with idiopathic thrombocytopenic purpura. *Br J Haematol*. 1996;95:732-737.
16. Asaka M, Kimura T, Kudo M, et al. Relationship of *Helicobacter pylori* to serum pepsinogen in an asymptomatic Japanese population. *Gastroenterology*. 1992;102:760-766.
17. Ohara S, Kato M, Asaka M, Toyota T. Studies of ^{13}C-urea breath test for diagnosis of *Helicobacter pylori* infection in Japan. *J Gastroenterol*. 1998;33:6-13.
18. Vianelli N, Valdre L, Fiacchini M, et al. Long-term follow-up of idiopathic thrombocytopenic purpura in 310 patients. *Haematologica*. 2001;86:504-509.
19. Yamamoto K, Sakoda H, Nakajima T, et al. Accumulation of multiple T cell clonotypes in the synovial lesions of patients with rheumatoid arthritis revealed by a novel clonality analysis. *Int Immunol*. 1992;4:1219-1223.
20. Chomczynski P, Sacchi N. Single-step method of RNA isolation by acid guanidinium thiocyanate-phenol-chloroform extraction. *Anal Biochem*. 1987;162:156-159.
21. Choi YW, Kotzin B, Herron L, Callahan J, Marrack P, Kappler J. Interaction of *Staphylococcus aureus* toxin "superantigens" with human T cells. *Proc Natl Acad Sci U S A*. 1989;86:8941-8945.
22. Gasbarrini A, Franceschi F. Autoimmune disease and *Helicobacter pylori* infection. *Biomed Pharmacother*. 1999;53:223-226.
23. Zentilin P, Seriolo B, Dulbecco P, et al. Eradication of *Helicobacter pylori* may reduce disease severity in rheumatoid arthritis. *Aliment Pharmacol Ther*. 2002;16:1291-1299.
24. Figura N, Giordano N, Burroni D, et al. Sjögren's syndrome and *Helicobacter pylori* infection. *Eur J Gastroenterol Hepatol*. 1994;6: 321-322.
25. de Luis DA, Varela C, de La Calle H, et al. *Helicobacter pylori* infection is markedly increased in patients with autoimmune atrophic thyroiditis. *J Clin Gastroenterol*. 1998;26:259-263.
26. Takahashi T, Yujiri T, Shinohara K, et al. Molecular mimicry by *Helicobacter pylori* CagA protein may be involved in the pathogenesis of *H. pylori*-associated chronic idiopathic thrombocytopenic purpura. *Br J Haematol*. 2004;124:91-96.
27. Olsson B, Andersson PO, Jernas M, et al. T-cell-mediated cytotoxicity toward platelets in chronic idiopathic thrombocytopenic purpura. *Nat Med*. 2003;9:1123-1124.

Develop. Growth Differ. (2006) **48**, 177–188 doi: 10.1111/j.1440-169x.2006.00855.x

Peroxisome proliferator-activated receptor γ ligands stimulate myeloid differentiation and lipogenesis in human leukemia NB4 cells

Etsuko Yasugi,[1,*] Akiko Horiuchi,[3] Isao Uemura,[4] Emiko Okuma,[1] Masami Nakatsu,[1] Kumiko Saeki,[1] Yasushi Kamisaka,[6] Hiroyuki Kagechika,[5] Kazuki Yasuda[2] and Akira Yuo[1]

Departments of [1]Hematology and [2]Metabolic Disorder, Research Institute, International Medical Center of Japan, 1-21-1, Toyama, Shinjuku-ku, Tokyo 162-8655, [3]Division of Natural Sciences, International Christian University, 3-10-2, Osawa, Mitaka-shi, Tokyo 181-8585, [4]Department of Biological Science, Graduate School of Science, Tokyo Metropolitan University, 1-1, Minamiosawa, Hachioji, Tokyo 192-0397, [5]School of Biomedical Science, Tokyo Medical and Dental University, 2-3-10 Kanda-Surugadai, Chiyoda-ku, Tokyo 101-0062, and [6]Lipid Engineering Research Group, Research Institute of Biological Resources, National Institute of Advanced Industrial Science and Technology, Tsukuba, Ibaraki 305-8566, Japan

Peroxisome proliferator-activated receptor γ (PPARγ) plays a central role in adipocyte and macrophage differentiation. Pioglitazone (Actos, AD4833), an antidiabetic drug, and 15-deoxy-$\Delta^{12,14}$-prostaglandin J2 (PGJ2) have recently been identified as synthetic and natural ligands for PPARγ, respectively. In this study, we examined the effects of PPARγ ligands on differentiation and lipogenesis in promyelocytic leukemia NB4 cells, in which PPARγ protein was expressed and ligand-stimulated PPARγ-specific transcription of adipocyte fatty-acid binding protein was confirmed. Treatment with PPARγ ligand (AD4833 or PGJ2) alone markedly suppressed proliferation but did not induce differentiation. The combined treatment of the cells with PPARγ ligand and all-trans retinoic acid (ATRA) synergistically induced myelocytic differentiation, as determined by nitroblue tetrazolium reducing ability and cell morphology. During these processes of differentiation, we observed marked accumulation of lipid droplets in the cytoplasm. The cellular triacylglycerol levels increased 2.7-fold after treatment with the inducers. Simultaneously, BODIPY-fatty acid was incorporated into the cytosol and concentrated in lipid droplets. The biosynthesis of triacylglycerol-containing BODIPY-fatty acids was increased twofold in differentiated cells. These findings clearly demonstrate that treatment with PPARγ ligands not only induced differentiation but also stimulated lipogenesis in NB4 cells, indicating a close association between differentiation and lipogenesis in PPARγ-stimulated human myeloid cells.

Key words: differentiation, lipogenesis, NB4 cell, pioglitazone, PPARγ ligand.

Introduction

Peroxisome proliferator-activated receptor γ (PPARγ) is a member of the nuclear receptor superfamily and is a ligand-dependent transcription factor (Kliewer *et al.* 1992a; Kliewer *et al.* 1992b). This receptor functions as a central regulator in the process of adipocyte or macrophage differentiation as well as in lipid and glucose metabolism (Nagy *et al.* 1998; Tontonoz *et al.* 1998; Rosen *et al.* 1999). Its ligands include modified fatty acids, the prostaglandin D2 metabolite 15-deoxy-$\Delta^{12,14}$-prostaglandin J2 (PGJ2), and antidiabetic drugs such as thiazolidione, rosiglitazone or pioglitazone (Forman *et al.* 1995; Lehmann *et al.* 1995; Nagy *et al.* 1998). PPARγ binds to DNA as a heterodimer with the retinoid X receptor (RXR). This heterodimer is also activated by RXR ligands (Kliewer *et al.* 1992b; Gearing *et al.* 1993). Together, ligands specific for PPARγ and RXR can synergistically activate transcription and promote adipocyte differentiation in culture (Schulman *et al.* 1998; Thuillier *et al.* 1998).

In several myelocytic cell lines, such as HL-60, U937 and NB4, all-trans retinoic acid (ATRA), which binds to retinoic acid receptors (RAR), induces differentiation of these immature myeloid cells into mature phagocytic cells (Breitman *et al.* 1980; Hu *et al.* 1993). ATRA has

Etsuko Yasugi and Akiko Horiuchi contributed equally to this work.

*Author to whom all correspondence should be addressed.
Email: e-yasugi@umin.ac.jp

Received 5 December 2005; revised 18 January 2006; accepted 19 January 2006.

been used successfully for the treatment of patients with acute promyelocytic leukemia (APL; Huang *et al.* 1988; Degos 1992). However, this therapy has one problem, that is, the prolonged use of a high dose of ATRA provoked expression of cytosolic retinoic acid-binding proteins, which resulted in the leukemic cells becoming resistant to the induction of differentiation (Cornic *et al.* 1992). 9-*cis*-Retinoic acid (9-*cis* RA), an isomer of ATRA that can bind both RAR and RXR, also proved to be potent in inducing differentiation (Kizaki *et al.* 1993; Sakashita *et al.* 1993). In addition, Evans *et al.* reported that the combination of a PPARγ ligand and an RXRα ligand induced monocytic differentiation of some myeloid leukemia cell lines (HL-60 and THP-1) (Nagy *et al.* 1998; Tontonoz *et al.* 1998). Therefore, we considered that the combination of PPARγ ligands with retinoids, not only RXR ligands but also RAR ligands, might have synergetic effects on differentiation in the APL cell line NB4.

Peroxisome proliferator-activated receptor γ functions as a transcriptional regulator of genes related to lipid metabolism. Known targets of PPARγ include the genes encoding adipocyte fatty acid binding protein (aP2), phosphoenoylpyruvate carboxykinase, lipoprotein lipase, and the brown fat uncoupling protein UCP1 (Tontonoz *et al.* 1998). PPARγ is expressed at high levels in adipose tissues and serves as a central regulator of the process of adipocyte differentiation (Chawla *et al.* 1994; Tontonoz *et al.* 1994). This transcription factor may also play an important role in the regulation of lipid metabolism in other cell types, such as cells in mammary and colonic epithelia (Mueller *et al.* 1998) and monocyte/macrophages (Tontonoz *et al.* 1998). These facts led us to study the effects of PPARγ ligands in combination with a retinoid on lipogenesis in human myeloid NB4 cells.

In this study, we investigated the combined effects of ATRA (RAR ligand) and PPARγ ligands on human myeloid NB4 cells. Two major cell biological phenomena on which we focused were differentiation and lipogenesis, since RAR and PPARγ play important roles in both of these biological phenomena in human myeloid cells, and therefore we can explore possible linkage between them in our *in vitro* assay system. Our data showed that pioglitazone or PGJ2 in conjunction with ATRA inhibited clonal proliferation and potently induced the differentiation of NB4 cells to granulocytic maturation. Furthermore, cells exposed to the combination of PPARγ ligand and ATRA accumulated lipid droplets. The levels and biosynthesis of triacylglycerol in the cells increased markedly after differentiation. Taken together, these findings show that treatment with PPARγ ligand and ATRA exerted synergistic effects on differentiation and lipogenesis in NB4 cells.

Materials and methods

Chemicals

All-trans retinoic acid, PGJ2, and the synthetic PPARγ ligand pioglitazone (Actos, AD4833) were obtained from Sigma-Aldrich (St Louis, MO, USA), Cayman Chemical (Ann Arbor, MI, USA) and Takeda Chemical Industries, (Tokyo, Japan), respectively. These reagents were dissolved in ethanol. PPARγ antagonist (GW9662), RXR antagonist (HX531) and RXR agonists (LG100268, PA024) were synthesized (Boehm *et al.* 1995; Ebisawa *et al.* 1999; Ohta *et al.* 2000; Willson *et al.* 2001). PPARγ antagonist (BADGE) was obtained from Cayman Chemicals. All antagonists and agonists were dissolved in ethanol. Diluent alone had no effect on the proliferation or differentiation of leukemia cell lines. BODIPY FL dodecanoic acid (BODIPY-FL-C12), cholesteryl BODIPY FL C12 and nile red were from Molecular Probes (Eugene, OR, USA). Triacylglycerol-containing BODIPY-FL-C12 was synthesized from 1, 2-diacylglyceride (Funakoshi Co., Tokyo, Japan) and BODIPY-FL-C12 using Lipase D derived from Rhizopus delemar (Amano Pharmaceutical Co., Nagoya, Japan). Anti-PPARγ (H-100) antibody was obtained from Santa-Cruz Biotechnology (Santa Cruz, CA, USA).

Cell culture

Human myelocytic leukemia cell lines (NB4 and HL-60) were grown in RPMI-1640 medium (Sigma-Ardrich) with 10% fetal calf serum (FCS; JRH Biosciences, Lenexa, KS, USA) at 37°C in an atmosphere of 5% CO_2. Cell suspension (4×10^4 cells/mL) in RPMI-1640 medium containing 10% FCS was placed in each well of 6-well plates or 24-well plates. PPARγ ligand and ATRA were added to the culture medium. The cells were incubated for the indicated periods and harvested for experiments. To examine the effect of antagonists, the cells were pretreated with antagonist for 8 h prior to treatment.

Assessment of cell proliferation and differentiation

Cell growth after various treatments was assessed by counting viable cells under a phase contrast microscope (Olympus CK40; Olympus, Tokyo, Japan). Differentiation of leukemia cells was examined by assessing their ability to produce superoxide, as measured by reduction of nitroblue tetrazolium (NBT; Nacarai Tesque, Kyoto, Japan). For analysis of the ability to reduce NBT, samples of cultured cells were washed once and then suspended in RPMI-1640 medium supplemented with 10% FCS containing 1 mg/mL NBT and 100 ng/mL 12-O-tetradecanoylphorbol 13-acetate (Sigma) for 30 min at 37°C. Cells containing

formazan blue-black deposits were detected light microscopy (Olympus BX-51) and counted. To further confirm cell differentiation, cytocentrifuged preparations of cells were stained with Wright-Giemsa solution and observed under a light microscope.

Ultrastructural analysis

For morphological observation of differentiation and lipid droplets, electron microscopy was used. Methods of fixation, staining, embedding and sectioning were described previously (Yasugi *et al.* 2002). Sections were examined with an electron microscope (JEOL JEM1010; JEOL, Tokyo, Japan) and images were taken with the Imaging Plate system (PIX system 20; JEOL).

Preparation of cell lysates, gel electrophoresis and immunoblotting

Cell pellets were suspended in 1× sample buffer and mixed vigorously. The cell suspension was heated for 5 min at 100°C and then frozen at –20°C until use. Proteins were separated by electrophoresis in a 10% sodium dodecyl sulfate–polyacrylamide gel and transferred to a polyvinylidene difluoride membrane in blotting buffer. After transfer, the membrane was blocked with 5% non-fat dry milk in phosphate-buffered saline (PBS) for 1 h at room temperature. After incubation with primary antibody against PPARγ, horseradish peroxidase-conjugated secondary antibody followed by the enhanced chemiluminescence (ECL) system from Amersham Biosciences (Piscataway, NJ, USA) were used for detection.

RNA analysis

Total RNA was obtained from cells using an RNeasy mini kit (QIAGEN, Hilden, Germany). The first strand cDNA was synthesized from 1 μg of total RNA using the Super Script II Transcriptase (Invitrogen Japan, Tokyo, Japan). For the polymerase chain reaction (PCR) assay, 1 μL of cDNA was used in a total volume of 50 μL containing 1× reaction buffer, 0.2 mM dNTP, 20 pmol of each primer, and 0.25 U of Ex Taq polymerase (Takara Bio., Otsu, Japan). PCR was performed in a GeneAmp PCR system 9600 (Applied Biosystems, Foster City, CA, USA) with the following temperature profile: denaturation at 95°C, primer annealing at 55°C, and primer extension at 72°C, each for 30 s. After an initial denaturation (95°C, 5 min), the cycle was performed 30 times, followed by a final extension step for 7 min at 72°C. The primers used for aP2 (Genbank accession number J02874) were as follows: sense primer, 5′-TCCAGTGAAAACTTTGATGATTAT-3′; antisense primer, 5′-ACGCATTCCACCACCAGTTTA-3′); as described before (Zilberfarb *et al.* 2001). The expected size of the PCR product was 320 bp. PCR products were visualized on a 2% agarose gel by ethidium bromide staining.

Lipid droplet staining in cells

Cells were fixed with 1% paraformaldehyde in PBS for 30 min at room temperature and washed with PBS. For detection of lipid droplets, the cells were stained with nile red at a final concentration of 0.1 μg/mL for 30 min at room temperature, and examined with a fluorescence microscope (Olympus BX-51). The cell morphology in the same fluorescent image was observed under a light microscope with Nomarski differential interference contrast (DIC). The fluorescent and DIC images of cells were captured by Aquacosmos (version 2.01) from a digital camera C4742-95 (Hamamatsu Photonics, Hamamatsu, Japan).

Quantitation of triacylglycerol

Each sample of cells was harvested after 4 days of treatment with PPARγ ligand and ATRA, and sonicated in water. Lipids were extracted from the homogenate with methanol–chloroform–water (2:1:0.8, v/v). Extracted lipid was evaporated to dryness and dissolved in chloroform–methanol (2:1, v/v). Total lipid was applied to a high performance thin-layer chromatography (HPTLC) silica gel plate (Kieselgel 60; Merk & Co., Whitehouse Station, NJ, USA). For detection of neutral lipid, the plate was developed with a solvent mixture of hexane–ethylacetate (1:1, v/v) and was stained with Morstein reagent (10% sulfuric acid solution containing 0.1% cesium sulfate and 5% ammonium pentamolybdate). Levels of triacylglycerol in cells were quantified enzymatically using a Triglyceride *G*-test Wako kit (Wako Pure Chemical Industries, Osaka, Japan).

Metabolism of fluorescent fatty acid analogues in NB4 cells

After treatment with PPARγ ligand and ATRA for 3 days, cells in 96-well plates were incubated in RPMI medium containing BODIPY-FL-C12 (10 ng/mL) for 2 min at room temperature. After washing, cells were subsequently chased in RPMI medium at room temperature for various periods and examined using a fluorescence microscope. The intensity of incorporated BODIPY-FL-C12 fluorescence in the cells was analyzed using a FluorImager 595 (Amersham Biosciences).

For detection of triacylglycerol synthesis, cells were incubated with BODIPY-FL-C12 for 10 min at room temperature, washed and further incubated for

30 min at 37°C. Lipids extracted from the cells were separated on HPTLC plates with a solvent mixture of hexane–diethylether (1:1, v/v), visualized using a FluorImager 595, and quantified as percentage using Image Quant software.

Triacylglycerol synthesis was assayed *in vitro* in a final volume of 300 μL containing 16 μM BODIPY-FL-C12, 36 μM coenzyme A sodium salt, 0.5 M Tris-HCl buffer (pH 7.5) and cell homogenate (125 μg of protein) as an enzyme source. Glycerol and dihydroxyacetone phosphate lithium salt were used as substrates. Incubation was carried out for 30 min at room temperature and terminated by the addition of 2 mL of ethyl acetate. Lipids were extracted twice with ethyl acetate for 2 min by vigorously shaking. Then the combined organic phases were applied to HPTLC plates. Triacylglycerol containing BODIPY-FL-C12 was visualized with a FluorImager 595 and its amount was estimated as described above.

Protein determination

Protein content was measured using the BCA Protein Assay Reagent (Pierce, Rockford, IL, USA).

Statistical analysis

Statistical significance was determined by using Student's *t*-test (two-tailed) to compare the two groups of data sets. Asterisks shown in the figures and tables indicate significant differences between experimental conditions and the corresponding control condition.

Results

Presence of peroxisome proliferator-activated receptor γ protein and the growth-suppressive effect of peroxisome proliferator-activated receptor γ ligands in myeloid cells

Peroxisome proliferator-activated receptor γ protein in untreated and differentiated NB4 cells was detected by western blotting. The relative molecular mass of the PPARγ protein was 52 KDa. The expression of PPARγ protein was found in untreated cells. Treatment with PPARγ ligand alone or with a combination of PPARγ ligand and ATRA for 2 days (Fig. 1) or 4 days (data not shown) resulted in expression levels equivalent to those in untreated cells.

The effects of PPARγ ligand and ATRA on the proliferation of NB4 cells are shown in Table 1. PPARγ ligand (PGJ2 (4 μM) or AD4833 (50 μM)) alone caused a dramatic decrease of cell growth after 4 days of incubation, though ATRA (1 nM) had less effect. Combined treatment with ATRA plus PGJ2 or AD4833 caused a further decrease in the number of viable cells.

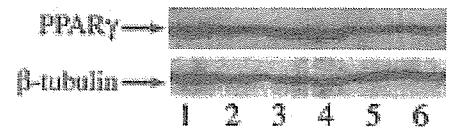

Fig. 1. Intracellular levels of peroxisome proliferator-activated receptor γ (PPARγ) protein in NB4 cells. Cells were treated with PPARγ ligand and/or all-trans retinoic acid (ATRA) for 2 days, and then whole cell extracts were subjected to western blot analysis. 1, Control; 2, 1 μM ATRA; 3, 4 μM 15-deoxy-Δ12,14-prostaglandin J2 (PGJ2); 4, 50 μM AD4833; 5, 1 μM ATRA + 4 μM PGJ2; 6, 1 μM ATRA + 50 μM AD4833.

Table 1. Effects of peroxisome proliferator-activated receptor γ ligands on NB4 cell growth

Treatment	Cell number (×10⁴)
Untreated	106.0 ± 4.3
1 nM ATRA	79.5 ± 3.5
4 μM PGJ2	34.7 ± 2.6
50 μM AD4833	47.0 ± 5.2
1 nμ ATRA + 4 μM PGJ2	26.7 ± 0.9
1 nM ATRA + 50 μM AD4833	31.7 ± 3.3

Cell number was counted after 4 days of treatment. Values are mean ± SD. ATRA, all-trans retinoic acid; PGJ2, 15-deoxy-Δ12,14-prostaglandin J2.

Peroxisome proliferator-activated receptor γ ligand and all-trans retinoic acid cooperate to promote NB4 differentiation

The differentiation of NB4 cells was evaluated by assessing the ability to reduce NBT, Wright-Giemsa staining and electron microscopic observation. With regard to NBT-reducing activity, neither PGJ2 nor AD4833 alone increased the activity of cells (data not shown). The combined treatment of cells with ATRA (1 nM) and PPARγ ligand strongly enhanced the NBT-reducing activity. More than 90% of cells treated with PPARγ ligand plus ATRA cells were positive for this activity, although ATRA-treated cells showed only 22% positivity (Fig. 2a). A high concentration of ATRA (1 μM) alone resulted in 96% of the cells being positive for NBT-reducing activity. In HL-60 cells, similar effects of PPARγ ligands and ATRA on differentiation were observed, although treatment with PGJ2 or AD4833 alone induced differentiation in these cells (Fig. 2b).

Next, the granulocytic differentiation of NB4 cells was morphologically confirmed by Wright-Giemsa staining (Fig. 3A). The cells treated with ATRA (1 nM) and PPARγ ligand showed lobulated kidney-bean or

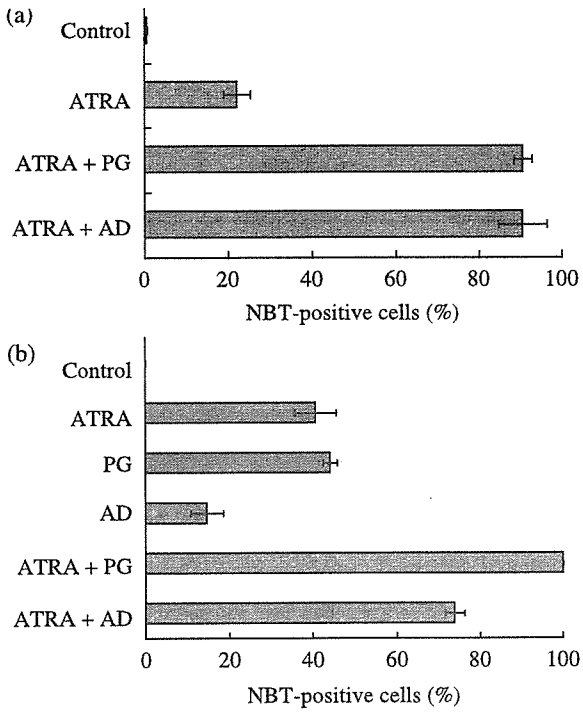

Fig. 2. Effects of peroxisome proliferator-activated receptor γ (PPARγ) ligands on nitroblue tetrazolium (NBT)-reducing activity in human myeloid cells. The NBT-reducing activities of NB4 (a) and HL-60 cells (b) were determined after 4 days of treatment with the indicated reagents. The activities are expressed as the percentage of NBT-positive cells. Results are representative of three experiments and are expressed as mean ± SD. (a) ATRA, 1 nM all-trans retinoic acid (ATRA); PG, 4 μM 15-deoxy-Δ12,14-prostaglandin J2 (PGJ2); AD, 50 μM AD4833. (b) ATRA, 1 μM ATRA; PG, 4 μM PGJ2; AD, 50 μM AD4833.

horse-shoe-shaped nuclei that are characteristic of granulocytes. The cytoplasm of those cells contained many white vacuoles and was stained white, in contrast to the blue cytoplasm of control cells. Furthermore ultrastructural observation showed that the combined treatment of cells with PPARγ ligand and ATRA (1 nM) induced irregularly lobulated nuclei and condensation of heterochromatin along the nuclear membrane (Fig. 3B). These results clearly indicate that PPARγ ligand and ATRA showed synergistic effects on granulocytic differentiation of NB4 cells.

Effects of peroxisome proliferator-activated receptor γ and retinoid X receptor antagonists on differentiation of NB4 cells

To confirm that the differentiation of NB4 cells is mediated through the PPARγ pathway, we used antagonists of PPARγ and RXR, such as GW9662 (Willson *et al.* 2001), BADGE (Wright *et al.* 2000) and HX531. HX531 works as an RXR antagonist (Ebisawa *et al.* 1999) but also as a potential PPARγ/RXR inhibitor (Yamauchi *et al.* 2001). The effects of PPARγ and RXR antagonists were evaluated in terms of the induced-differentiation of NB4 cells as determined by the NBT reduction assay. Their effects on ATRA ligand- and PPARγ ligand-induced NB4 differentiation are summarized in Table 2. All three antagonists showed inhibitory effects on the differentiation induced by the combination of ATRA and PPARγ ligands. In contrast, PPARγ antagonists did not exert an inhibitory effect on the differentiation of NB4 cells induced by ATRA

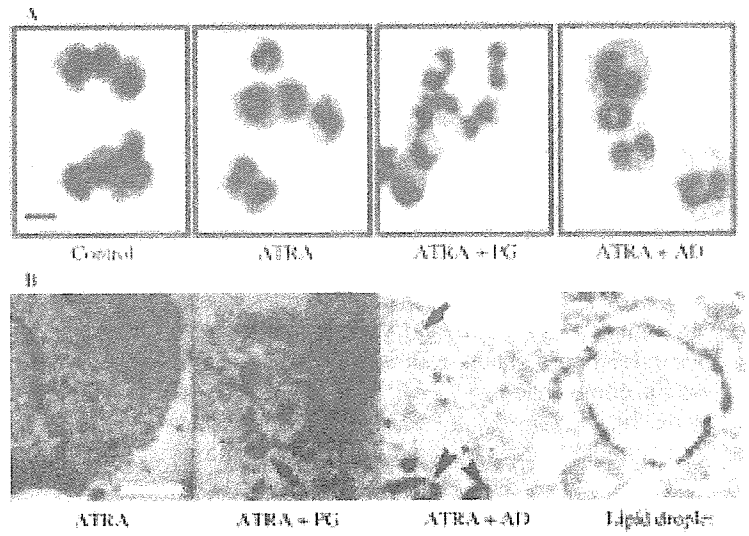

Fig. 3. Morphological observation of NB4 cells treated with peroxisome proliferator-activated receptor γ (PPARγ) ligand and/or all-trans retinoic acid (ATRA). The cells were treated for 4 days with ATRA (1 nM), PG (4 μM 15-deoxy-Δ12,14-prostaglandin J2), AD (50 μM AD4833), individually or combined. (A) Wright-Giemsa staining. Bar, 20 μm (B) Ultrastructural observation. Arrowhead and arrow indicate nucleus and lipid droplet, respectively. Bar, 4 μm. Right panel is higher magnification of the lipid droplet. Bar, 0.5 μm.

Table 2. Effects of peroxisome proliferator-activated receptor γ antagonists on NB4 differentiation

	None	HX531	GW9662	BADGE
1 μM ATRA	96.1 ± 2.2	95.0 ± 2.0	97.1 ± 0.2	94.3 ± 2.1
1 nM ATRA	22.0 ± 3.2	12.0 ± 2.2*	16.5 ± 8.8	25.5 ± 3.4
1 nM ATRA + 0.5 μM PGJ2	39.4 ± 4.9			28.7 ± 3.3*
1 nM ATRA + 2 μM PGJ2	91.7 ± 4.7	15.3 ± 1.0**	19.2 ± 3.8**	92.2 ± 2.1
1 nM ATRA + 50 μM AD4833	90.4 ± 5.8	3.2 ± 0.6***	5.6 ± 0.8***	26.3 ± 6.9**

Concentration of each antagonist was 1 μM. Values are expressed as percent of NBT-positive cells. Values are mean ± SD. Probabilities were calculated for the percentages of NBT-positive cells with and without peroxisome proliferator-activated receptor γ antagonist. *$P < 0.05$, **$P < 0.01$, ***$P < 0.001$. ATRA, all-trans retinoic acid; PGJ2, 15-deoxy-Δ ^{12,14}-prostaglandin J2.

Table 3. Effects of retinoic X receptor agonists on NB4 differentiation

	LG100268	PA024
None	0.8 ± 0.1	2.9 ± 0.7
4 μM PGJ2	74.8 ± 7.4***	26.3 ± 5.4**
50 μM AD4833	17.0 ± 1.3**	13.3 ± 3.5*

Concentration of each agonist was 1 μM. Values are expressed as percent of NBT-positive cells. Values are mean ± SD. Probabilities were calculated for the percentages of NBT-positive cells with and without peroxisome proliferator-activated receptor γ ligand. *$P < 0.05$, **$P < 0.01$, ***$P < 0.005$. PGJ2, 15-deoxy-Δ ^{12,14}-prostaglandin J2.

(1 nM or 1 μM) alone. Thus, for the induction of differentiation by the combination of ATRA and PPARγ ligands, the signaling through PPARγ/RXR is necessary. The combination of RXR agonist and PPARγ ligand also induced NB4 differentiation, indicating that the stimulation of the RXR receptor is important in this differentiation pathway (Table 3).

Upregulation of adipocyte fatty acid binding protein in NB4 cells during treatment with peroxisome proliferator-activated receptor γ ligands

The expression of adipocyte fatty acid binding protein (aP2), whose promoter has an adipose response element (ARE; DR-1), occurs in parallel to the expression of PPARγ (Thuillier *et al.* 1998). We examined the gene expression of aP2 in NB4 cells by reverse transcription–polymerase chain reaction (RT–PCR) after treatment with ATRA (1 μM) and PPARγ ligand (Fig. 4). The expression of aP2 mRNA was greatly induced after 24 h and continued for up to 4 days in NB4 cells cultured with PPARγ ligand alone or with a combination of PPARγ ligand and ATRA, whereas the expression of this gene remained low or undetectable in cells cultured with ATRA alone or in untreated cells. Thus, in human myeloid cells, PPARγ ligands induced the transcription of a gene

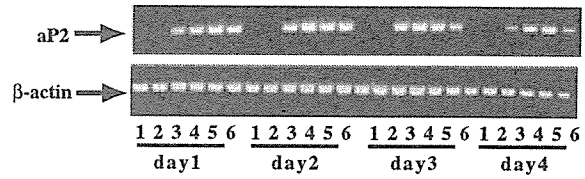

Fig. 4. Adipocyte fatty acid binding protein (aP2) mRNA expression in NB4 cells after treatment with peroxisome proliferator-activated receptor γ (PPARγ) ligand and/or all-trans retinoic acid (ATRA). Cells were treated with PPARγ ligand and/or ATRA for the indicated periods. Reverse transcription–polymerase chain reaction for aP2 mRNA in freshly prepared NB4 cells revealed a cDNA fragment of the expected size. 1, Control; 2, 1 μM ATRA; 3, 1 μM ATRA + 4 μM PGJ2; 4, 1 μM ATRA + 50 μM AD4833; 5, 4 μM PGJ2; 6, 50 μM AD4833. As a control for cDNA quality, the signals for β-actin expression are shown.

specific for this transcriptional receptor and important for lipid metabolism.

Lipid droplets accumulate in NB4 cells after treatment with peroxisome proliferator-activated receptor γ ligands and all-trans retinoic acid

In the cytoplasm of cells treated with PPARγ ligands and ATRA, we found many white vacuoles after Wright-Giemsa-staining, as mentioned above (Fig. 3A). We speculated that these vacuoles might be lipid droplets and examined the cells by fluorescence microscopy after staining with the lipophilic dye nile red. As nile red has the remarkable property of staining neutral lipids (Greenspan *et al.* 1985), lipid droplets containing triacylglycerol or cholesterol ester show a fluorescent red color. In Figure 5A, NB4 cells after treatment with PPARγ ligands and ATRA (1 μM) contained numerous nile red-positive droplets. In the cytoplasm of cells treated with ATRA alone, there were also lipid droplets, but the number of droplets was fewer and the intensity of the fluorescence was weaker. In the cells treated with PGJ2 or AD4833 alone, lipid droplets were weakly visible (data not

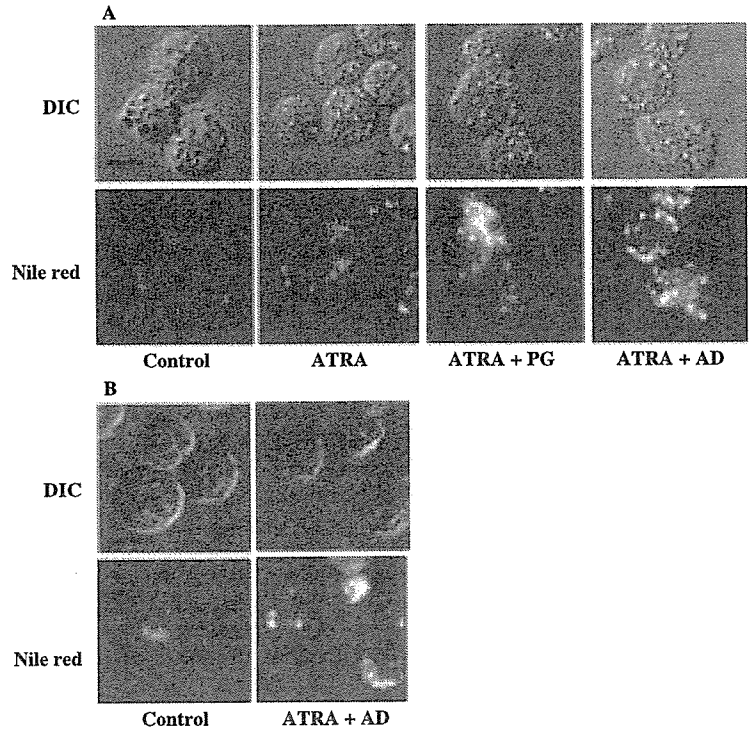

Fig. 5. Accumulation of lipid droplets in differentiated NB4 and HL-60 cells. Cells were treated for 4 days with all-trans retinoic acid (ATRA; 1 μM), ATRA (1 μM) + 15-deoxy-Δ12,14-prostaglandin J2 (PG; 4 μM) or ATRA (1 μM) + AD4833 (AD; 50 μM). Upper panels are difference interference contrast images, and lower panels are the corresponding images obtained by fluorescence microscopy. Lipid droplets were stained with nile red. Bar, 10 μm. (A) NB4 cells, (B) HL-60 cells.

shown). Similar findings were made in HL-60 cells (Fig. 5B). Ultrastructural observation revealed that treatment with PPARγ ligand and ATRA clearly stimulated the accumulation of lipid droplets in the cytoplasm (Fig. 3B). Lipid droplets are surrounded by a phospholipid monolayer, and clearly distinguished from other organelles in the cytoplasm. Both types of microscopic observation clearly demonstrated that PPARγ ligands stimulated the accumulation of lipid droplets in NB4 cells.

Triacylglycerol levels increase in NB4 cells after treatment with peroxisome proliferator-activated receptor γ ligands and all-trans retinoic acid

We examined whether treatment with PPARγ ligand and ATRA (1 μM) affected the cellular levels of triacylglycerol and cholesterol ester, the major storage lipids in mammalian cells. Thin-layer chromatography revealed that treatment with PPARγ ligand and ATRA particularly increased the triacylglycerol level in NB4 cells, and slightly increased the cholesterol ester level (Fig. 6a). Free-cholesterol levels were almost equivalent between untreated cells and cells treated with PPARγ ligand and ATRA. Next, the cellular triacylglycerol levels were analyzed enzymatically (Fig. 6b). After incubation with ATRA (1 μM) combined with PGJ2 or AD4833, the triacylglycerol level of NB4 cells was increased by 2.7-fold compared to that in untreated cells. PGJ2 or AD4833 alone also increased the triacylglycerol level slightly, but ATRA alone did not. These results strongly suggest that the lipid droplets in NB4 cells contained predominantly triacylglycerol, and the level of triacylglycerol increased after treatment of the cells with PPARγ ligand and ATRA.

Translocation of a fluorescent fatty acid analogue, BODIPY-FL-C12 in NB4 cells treated with peroxisome proliferator-activated receptor γ ligands and all-trans retinoic acid

The distribution pattern of intracellular BODIPY fluorescence was compared between differentiated and untreated cells under the pulse-chase conditions (Fig. 7a). After prelabeling of cells with BODIPY-FL-C12 at room temperature, intracellular fluorescence was distributed in the cytoplasm, including the endoplasmic reticulum (ER), in both differentiated and untreated cells. After a chase of 10–30 min, most of the intracellular fluorescence in differentiated cells was clearly accumulated in the lipid droplets, though that in untreated cells remained in the cytoplasm. The translocation of the fluorescence from the cytosol to lipid droplets was observed in differentiated cells treated with ATRA alone or with ATRA and PPARγ ligand. There was no significant difference in total

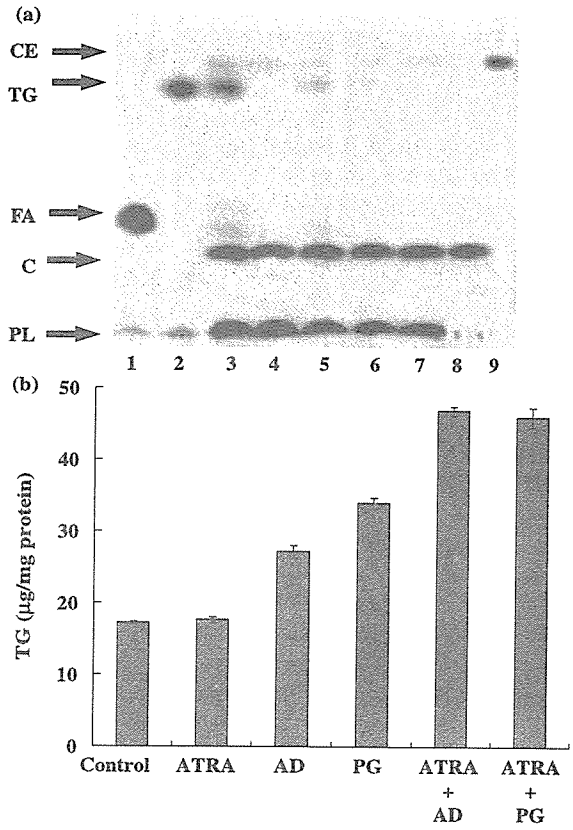

Fig. 6. (a) Thin-layer chromatogram of neutral lipids in differentiated NB4 cells. Each lane was spotted with crude lipid extracted from 7×10^4 cells. Cells were treated for 4 days with peroxisome proliferator-activated receptor γ (PPARγ) ligands and/or all-trans retinoic acid (ATRA). 1, linoleic acid; 2, trilinolein; 3, 1 μM ATRA + 4 μM 15-deoxy-Δ12,14-prostaglandin J2 (PGJ2); 4, control; 5, 1 μM ATRA + 50 μM AD4833; 6, 1 μM ATRA; 7, control; 8, cholesterol; 9, cholesterol ester. CE, cholesterol ester; TG, triacylglycerol; FA, fatty acid; C, cholesterol; PL, phospholipid. (b) Triacylglycerol levels in differentiated NB4 cells. Cells were treated for 4 days with PPARγ ligand and/or ATRA (1 μM). PG, 4 μM PGJ2; AD, 50 μM AD4833. Values represent mean ± SD. Triacylglycerol contents are expressed as μg/mg protein.

amount of BODIPY lipid associated with cells between the differentiated and untreated cells (data not shown). These observations provided evidence that BODIPY-FL-C12 was incorporated in the cytoplasm and immediately translocated to lipid droplets in differentiated cells.

Metabolism of BODIPY-FL-C12 in NB4 cells treated with peroxisome proliferator-activated receptor γ ligands and all-trans retinoic acid

In order to examine the metabolism of incorporated BODIPY-FL-C12, cells were prelabeled with BODIPY-FL-C12 at room temperature for 10 min and incubated for 30 min at 37°C. Extracted lipids containing BODIPY-FL-C12 were analyzed by thin-layer chromatography using a FluorImager. The fluorescent spots of triacylglycerol containing BODIPY-FL-C12 were detected in lipids extracted from both differentiated and untreated cells (data not shown). The Rf value of triacylglycerol containing BODIPY-FL-C12 was confirmed by the comigration of synthesized triacylglycerol containing BODIPY-FL-C12. The fluorescence of triacylglycerol extracted from cells treated with PPARγ ligands and ATRA was about twofold stronger than that of untreated cells (Fig. 7b). These findings indicated that BODIPY-FL-C12 had been incorporated in the cytoplasm and converted to triacylglycerol.

Triacylglycerol synthesis activity in differentiated and untreated cell homogenates was compared using two substrates, glycerol and dihydroxyacetone phosphate, respectively. The activity in differentiated cells treated with PPARγ ligands and ATRA was found to be more than twofold higher than that in untreated cells using glycerol as substrate (Fig. 7c). The activity was dependent on glycerol concentration (Fig. 7c) but not on dihydroxyacetone phosphate (data not shown).

These findings suggest that triacylglycerol was synthesized from glycerol in differentiated cells. Taken together, these data show that triacylglycerol synthesis in NB4 cells treated with PPARγ ligand and ATRA increased.

Discussion

Peroxisome proliferator-activated receptor γ has been demonstrated to regulate adipocyte differentiation and glucose homeostasis in response to several structurally distinct compounds, including thiazolidinediones (Tontonoz *et al.* 1994; Lehmann *et al.* 1995). In this study, we investigated the effects of PPARγ ligands on human NB4 and HL-60 cells and found that PPARγ ligands can act synergistically with ATRA to induce differentiation into cells that show granulocytic characteristics and accumulate lipid droplets. Activation of PPARγ in immortalized cell lines, such as THP-1 and HL-60, promotes differentiation along the macrophage lineage, as shown by changes in gene expression and uptake of OxLDL induced by CD36 (Hirase *et al.* 1999; Tontonoz *et al.* 1998). However, using PPARγ -deficient stem cells, Moore *et al.* demonstrated that PPARγ is neither essential for myeloid development nor for mature macrophage functions such as phagocytosis and inflammatory production (Moore *et al.* 2001). Furthermore, Asou *et al.* reported the effects of troglitazone on the proliferation and

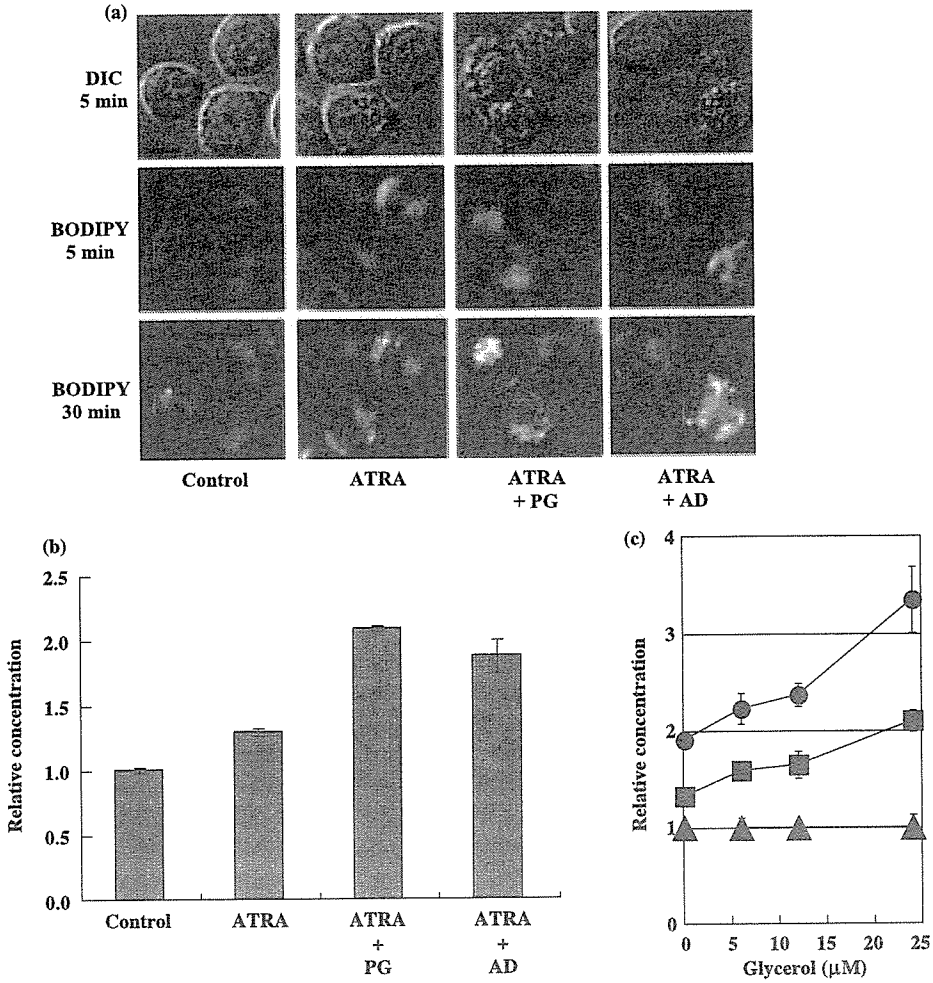

Fig. 7. (a) Intracellular distribution of BODIPY-FL-C12 fluorescence in differentiated and untreated NB4 cells. Cells were treated for 3 days with all-trans retinoic acid (ATRA; 1 μM), ATRA (1 μM) + 15-deoxy-Δ12,14-prostaglandin J2 (PG; 4 μM) or ATRA (1 μM) + AD (AD4833, 50 μM). Cells were incubated in medium containing BODIPY-FL-C12 for 2 min at room temperature and were subsequently chased and examined using a fluorescence microscope. Upper panels are difference interference contrast images. Middle and lower panels are the corresponding fluorescence microscopy images. BODIPY, BODIPY-FL-C12. Bar, 10 μm. (b) Relative concentration of triacylglycerol containing BODIPY-FL-C12 in NB4 cells. Cells were treated for 3 days with peroxisome proliferator-activated receptor γ (PPARγ) ligand (PGJ2 4 μM, AD4833 50 μM) and/or ATRA (1 μM). The assay methods are described in Materials and methods. Values represent mean ± SD. The relative concentrations of triacylglycerol containing BODIPY-FL-C12 in differentiated cells were calculated as fluorescence strength compared to that in untreated cells taken as 1.00. (c) Triacylglycerol synthesis activity in NB4 cells. Cells were treated for 3 days with PPARγ ligand (PGJ2 4 μM, AD4833 50 μM) and ATRA (1 μM). The method of the enzyme assay is described in Materials and methods. Values are mean ± SD. The relative concentrations of triacylglycerol containing BODIPY-FL-C12 in differentiated cells are plotted together with that of untreated cells taken as 1.00. (●), ATRA + PG; (■), ATRA + AD; (▲), control.

differentiation of normal and malignant myeloid cells (especially monocytic cells) and demonstrated that troglitazone combined with a retinoid was a moderately potent inhibitor of the clonogenic growth of acute myeloid leukemia cells, but not a potent inducer of differentiation of these leukemia cells (Asou *et al.* 1999). Our results clearly indicated that combined treatment with PPARγ ligand and ATRA induced differentiation of NB4 cells. This discrepancy between these findings may be related to the fact that in the study of Asou *et al.* (1999), NB4 cells were treated with troglitazone (10^{-5} M) as the PPARγ ligand, and the concentration of troglitazone was rather low compared to our conditions. We also examined the effects of PPARγ ligands and ATRA on HL-60 cells and observed synergistic effects of PPARγ ligands

on the induction of differentiation and lipogenesis, as in NB4 cells.

The basis for differentiation therapy of acute leukemia is the treatment of cells with several physiological agents at low concentration because high doses of single agents might provoke the side-effects of the agents and the resistance to the induction of differentiation. In this study, when PPARγ ligands were used alone, differentiation did not occur, but the combination of PPARγ ligand and ATRA synergistically promoted the differentiation of NB4 cells. The observed cooperativity between PPARγ ligands and ATRA has important implications for the use of combinations of these agents in differentiation therapy. PPARγ, like many members of the nuclear hormone receptor superfamily, functions as a heterodimer with the RXR. Recent studies have identified two types of RXR-dependent heterodimers: non-permissive and permissive (Schulman *et al.* 1998; Westin *et al.* 1998). In non-permissive heterodimers, such as those between RXR and RAR, the partner actively interferes with the ability of RXR-specific ligands. In contrast, permissive heterodimers, such as RXR-PPARγ, allow RXR signaling. In the current study, we demonstrated the synergistic effects of PPARγ ligands and ATRA on the differentiation of NB4 cells. The individual signaling pathways of RAR/RXR and PPARγ/RXR may have synergistically transduced signals for differentiation in NB4 cells. 9-*cis* RA, mono-*cis* isomers of retinoids, binds to RXR receptors in addition to RAR receptors and induces differentiation in HL-60 cells (Kizaki *et al.* 1993; Sakashita *et al.* 1993). However, 9-*cis* RA was clinically less effective for remission APL compared with ATRA. We did not perform experiments on the synergic effects of 9-*cis* RA with PPARγ ligands instead of ATRA in this study. Indeed, the duration of cell treatments being between 2 and 4 days, ATRA could be, at least partially, converted into 9-*cis* RA and 13-*cis* RA. In this case, the pathway of PPARγ/RXR may have induced differentiation by the synergic effects of 9-*cis* RA and PPARγ ligands. Further investigation will be needed to clarify this point.

In order to determine whether AD4833 or PGJ2 in fact binds PPARγ in NB4 cells, we examined the effects on differentiation using PPARγ or RXR antagonists. GW9662 and BADGE, both of which are specific PPARγ antagonists, significantly suppressed the differentiation of NB4 cells induced by PPARγ ligand and ATRA. The inhibitory effect of GW9662 was stronger than that of BADGE at the same concentration. Recently, Fehlberg *et al.* reported that high concentrations of BADGE induced apoptosis in tumor cells independently of PPARγ (Fehlberg *et al.* 2002). In our study, NB4 cells did not show apoptosis because we used a low concentration of agonist (data not shown). HX531 is an RXR antagonist but acts also as a potential inhibitor of PPARγ/RXR in an *in vitro* transactivation assay and to prevent triglyceride accumulation in 3T3L1 adipocytes (Yamauchi *et al.* 2001). HX531 significantly inhibited the differentiation of NB4 cells induced by PPARγ ligand and ATRA. Both PPARγ and RXR antagonists suppressed this differentiation, indicating that AD4833 and PGJ2 act on the cells via PPARγ/RXR receptor.

With regard to the effects of PPARγ ligands on the accumulation of lipid in the cytoplasm, several studies using rosiglitazone have found that PPARγ may promote macrophage lipid accumulation (Nagy *et al.* 1998; Tontonoz *et al.* 1998; Chawla *et al.* 2001). Recently, the opposite theory was proposed, namely that PPARγ activation by rosiglitazone is not related to lipid accumulation in macrophages (Chinetti *et al.* 2001; Moore *et al.* 2001; Vosper *et al.* 2001). Our findings were consistent with the former theory, that is, lipid droplets accumulated during differentiation in NB4 cells treated with PPARγ ligand and ATRA. The triacylglycerol levels in PPARγ ligand- and ATRA-treated cells were obviously higher than that in cells treated with ATRA alone (Fig. 6b). These findings suggest that PPARγ accelerated the formation of lipid droplets by upregulating gene expression related to lipogenesis in NB4 cells. We examined the enzyme activity of glycerol-3-phosphate dehydrogenase (GPDH; EC 1.1.1.8), and the expression of CD36 (scavenger receptor-class B, fatty acid translocase). However, there was no difference in the enzyme activity or protein expression between PPARγ ligand and ATRA-treated and untreated cells. CD36 expression was not detected by fluorescence activated cell sorting analysis in either untreated or treated cells (data not shown). On the other hand, expression of aP2 mRNA in NB4 cells was upregulated by PPARγ ligand treatments (Fig. 4).

Furthermore, to elucidate the features of lipogenesis during differentiation, we examined the incorporation of fluorescent fatty acids in the cytoplasm. The fluorescent analogue was rapidly converted to triacylglycerols and targeted to the lipid droplets in NB4 cells treated with PPARγ ligand and ATRA. Large lipid droplets from adipocytes, rich in triacylglycerols, are retained within the cells as a source of fatty acids for mitochondrial and peroxisomal oxidation to produce energy (Brasaemle *et al.* 1997). However, almost all other mammalian tissues examined contain small lipid droplets, which are less well characterized (Atshaves *et al.* 1998; Murphy & Vance 1999; Sparrow *et al.* 1999). Burns *et al.* reported that human neutrophils

take up much more fatty acid than lymphocytes primarily because they synthesize much larger quantities of triacylglycerols, a fatty acid storage form (Burns *et al.* 1976). It is postulated that lipid droplets may represent the storage form for free fatty acids which may be utilized for membrane synthesis during phagocytosis (Elsbach 1964; Elsbach & Farrow 1969; Lutas & Zucker-Franklin 1977). In these theories, the differentiation of phagocytes is accompanied by lipid droplet accumulation. We also examined the biosynthesis of triacylglycerols using fluorescent fatty acid. The results demonstrated that the rate of triacylglycerol synthesis is more than twofold greater in differentiated cells. From the results of triacylglycerol enzyme activity assays, we suggest that triacylglycerols are synthesized from glycerol but not dihydroxyacetone phosphate in PPARγ ligand- and ATRA-treated cells. In adipocytes, thiazolidinediones markedly induce glycerol kinase gene expression and stimulate the incorporation of glycerol rather than glucose into triacylglycerol (Guan *et al.* 2002). In the synthesis of glycerolipids, it is well established that glycerol has to be phosphorylated to glycerol-3-phosphate before acylation occurs. However, in the microsomal fraction of heart, liver, kidney, skeletal muscle and brain tissues, direct acylation of glycerol becomes more prominent when exogenous glycerol levels become elevated (Lee *et al.* 2001). Both of those reports are in accord with our conclusion that glycerol was used as substrate in triacylglycerol synthesis. Further investigations will be required to determine the relationship between differentiation and the accumulation of lipid droplets in acute myeloid leukemia treated with PPARγ ligands and ATRA.

Acknowledgement

We thank the Takeda Pharmaceutical Company (Tokyo, Japan) for providing AD4833.

References

Asou, H., Verbeek, W., Williamson, E. *et al.* 1999. Growth inhibition of myeloid leukemia cells by troglitazone, a ligand for peroxisome proliferator activated receptor γ, and retinoids. *Int. J. Oncol.* **15**, 1027–1031.

Atshaves, B. P., Foxworth, W. B., Frolov, A. *et al.* 1998. Cellular differentiation and I-FABP protein expression modulate fatty acid uptake and diffusion. *Am. J. Physiol.* **274**, C633–C644.

Boehm, M. F., Zhang, L., Zhi, L. *et al.* 1995. Design and synthesis of potent retinoid X receptor selective ligands that induce apoptosis in leukemia cells. *J. Med. Chem.* **38**, 3146–3155.

Brasaemle, D. L., Barber, T., Wolins, N. E., Serrero, G., Blanchette-Mackie, E. J. & Londos, C. 1997. Adipose differentiation-related protein is an ubiquitously expressed lipid storage droplet-associated protein. *J. Lipid Res.* **38**, 2249–2263.

Breitman, T. R., Selonick, S. E. & Collins, S. J. 1980. Induction of differentiation of the human promyelocytic leukemia cell line (HL-60) by retinoic acid. *Proc. Natl Acad. Sci. USA* **77**, 2936–2940.

Burns, C. P., Welshman, I. R. & Spector, A. A. 1976. Differences in free fatty acid and glucose metabolism of human blood neutrophils and lymphocytes. *Blood* **47**, 431–437.

Chawla, A., Barak, Y., Nagy, L., Liao, D., Tontonoz, P. & Evans, R. M. 2001. PPAR-γ dependent and independent effects on macrophage-gene expression in lipid metabolism and inflammation. *Nat. Med.* **7**, 48–52.

Chawla, A., Schwarz, E. J., Dimaculangan, D. D. & Lazar, M. A. 1994. Peroxisome proliferator-activated receptor (PPAR) γ: adipose-predominant expression and induction early in adipocyte differentiation. *Endocrinology* **135**, 798–800.

Chinetti, G., Lestavel, S., Bocher, V. *et al.* 2001. PPAR-α and PPAR-γ activators induce cholesterol removal from human macrophage foam cells through stimulation of the ABCA1 pathway. *Nat. Med.* **7**, 53–58.

Cornic, M., Delva, L., Guidez, F., Balitrand, N., Degos, L. & Chomienne, C. 1992. Induction of retinoic acid-binding protein in normal and malignant human myeloid cells by retinoic acid in acute promyelocytic leukemia patients. *Cancer Res.* **52**, 3329–3334.

Degos, L. 1992. Retinoic acid in acute promyelocytic leukemia: a model for differentiation therapy. *Curr. Opin. Oncol.* **4**, 45–52.

Ebisawa, M., Umemiya, H., Ohta, K. *et al.* 1999. Retinoid X receptor-antagonistic diazepinylbenzoic acids. *Chem. Pharm. Bull. (Tokyo)* **47**, 1778–1786.

Elsbach, P. 1964. Comparison of Uptake of Palmitic, Stearic, Oleic and Linoleic Acid by Polymorphonuclear Leukocytes. *Biochim. Biophys. Acta* **84**, 8–17.

Elsbach, P. & Farrow, S. 1969. Cellular triglyceride as a source of fatty acid for lecithin synthesis during phagocytosis. *Biochim. Biophys. Acta* **176**, 438–441.

Fehlberg, S., Trautwein, S., Goke, A. & Goke, R. 2002. Bisphenol A diglycidyl ether induces apoptosis in tumour cells independently of peroxisome proliferator-activated receptor-γ, in caspase-dependent and -independent manners. *Biochem. J.* **362**, 573–578.

Forman, B. M., Tontonoz, P., Chen, J., Brun, R. P., Spiegelman, B. M. & Evans, R. M. 1995. 15-Deoxy-Δ 12, 14-prostaglandin J2 is a ligand for the adipocyte determination factor PPAR γ. *Cell* **83**, 803–812.

Gearing, K. L., Gottlicher, M., Teboul, M., Widmark, E. & Gustafsson, J. A. 1993. Interaction of the peroxisome-proliferator-activated receptor and retinoid X receptor. *Proc. Natl Acad. Sci. USA* **90**, 1440–1444.

Greenspan, P., Mayer, E. P. & Fowler, S. D. 1985. Nile red: a selective fluorescent stain for intracellular lipid droplets. *J. Cell Biol.* **100**, 965–973.

Guan, H. P., Li, Y., Jensen, M. V., Newgard, C. B., Steppan, C. M. & Lazar, M. A. 2002. A futile metabolic cycle activated in adipocytes by antidiabetic agents. *Nat. Med.* **8**, 1122–1128.

Hirase, N., Yanase, T., Mu, Y. *et al.* 1999. Thiazolidinedione induces apoptosis and monocytic differentiation in the promyelocytic leukemia cell line HL60. *Oncology* **57** (Suppl. 2), 17–26.

Hu, Z. B., Ma, W., Uphoff, C. C., Lanotte, M. & Drexler, H. G. 1993. Modulation of gene expression in the acute promyelocytic leukemia cell line NB4. *Leukemia* **7**, 1817–1823.

Huang, M. E. Ye, Y. C., Chen, S. R. *et al.* 1988. Use of all-trans retinoic acid in the treatment of acute promyelocytic leukemia. *Blood* **72**, 567–572.

Kizaki, M., Ikeda, Y., Tanosaki, R. *et al.* 1993. Effects of novel retinoic acid compound, 9-cis-retinoic acid, on proliferation, differentiation, and expression of retinoic acid receptor-α and retinoid X receptor-α RNA by HL-60 cells. *Blood* **82**, 3592–3599.

Kliewer, S. A., Umesono, K., Mangelsdorf, D. J. & Evans, R. M. 1992a. Retinoid X receptor interacts with nuclear receptors in retinoic acid, thyroid hormone and vitamin D3 signalling. *Nature* **355**, 446–449.

Kliewer, S. A., Umesono, K., Noonan, D. J., Heyman, R. A. & Evans, R. M. 1992b. Convergence of 9-cis retinoic acid and peroxisome proliferator signalling pathways through heterodimer formation of their receptors. *Nature* **358**, 771–774.

Lee, D. P., Deonarine, A. S., Kienetz, M. *et al.* 2001. A novel pathway for lipid biosynthesis: the direct acylation of glycerol. *J. Lipid Res.* **42**, 1979–1986.

Lehmann, J. M., Moore, L. B., Smith-Oliver, T. A., Wilkison, W. O., Willson, T. M. & Kliewer, S. A. 1995. An antidiabetic thiazolidinedione is a high affinity ligand for peroxisome proliferator-activated receptor γ (PPAR γ). *J. Biol. Chem.* **270**, 12 953–12 956.

Lutas, E. M. & Zucker-Franklin, D. 1977. Formation of lipid inclusions in normal human leukocytes. *Blood* **49**, 309–320.

Moore, K. J., Rosen, E. D., Fitzgerald, M. L. *et al.* 2001. The role of PPAR-γ in macrophage differentiation and cholesterol uptake. *Nat. Med.* **7**, 41–47.

Mueller, E., Sarraf, P., Tontonoz, P. *et al.* 1998. Terminal differentiation of human breast cancer through PPAR γ. *Mol. Cell* **1**, 465–470.

Murphy, D. J. & Vance, J. 1999. Mechanisms of lipid-body formation. *Trends Biochem. Sci.* **24**, 109–115.

Nagy, L., Tontonoz, P., Alvarez, J. G., Chen, H. & Evans, R. M. 1998. Oxidized LDL regulates macrophage gene expression through ligand activation of PPAR γ. *Cell* **93**, 229–240.

Ohta, K., Kawachi, E., Inoue, N. *et al.* 2000. Retinoidal pyrimidinecarboxylic acids. Unexpected diaza-substituent effects in retinobenzoic acids. *Chem. Pharm. Bull. (Tokyo)* **48**, 1504–1513.

Rosen, E. D., Sarraf, P., Troy, A. E. *et al.* 1999. PPAR γ is required for the differentiation of adipose tissue in vivo and in vitro. *Mol. Cell* **4**, 611–617.

Sakashita, A., Kizaki, M., Pakkala, S. *et al.* 1993. 9-cis-retinoic acid: effects on normal and leukemic hematopoiesis in vitro. *Blood* **81**, 1009–1016.

Schulman, I. G., Shao, G. & Heyman, R. A. 1998. Transactivation by retinoid X receptor-peroxisome proliferator-activated receptor γ (PPAR γ) heterodimers: intermolecular synergy requires only the PPAR γ hormone-dependent activation function. *Mol. Cell Biol.* **18**, 3483–3494.

Sparrow, C. P., Patel, S., Baffic, J. *et al.* 1999. A fluorescent cholesterol analog traces cholesterol absorption in hamsters and is esterified in vivo and in vitro. *J. Lipid. Res.* **40**, 1747–1757.

Thuillier, P., Baillie, R., Sha, X. & Clarke, S. D. 1998. Cytosolic and nuclear distribution of PPAR γ 2 in differentiating 3T3-L1 preadipocytes. *J. Lipid Res.* **39**, 2329–2338.

Tontonoz, P., Hu, E. & Spiegelman, B. M. 1994. Stimulation of adipogenesis in fibroblasts by PPAR γ 2, a lipid-activated transcription factor. *Cell* **79**, 1147–1156.

Tontonoz, P., Nagy, L., Alvarez, J. G., Thomazy, V. A. & Evans, R. M. 1998. PPAR γ promotes monocyte/macrophage differentiation and uptake of oxidized LDL. *Cell* **93**, 241–252.

Vosper, H., Patel, L., Graham, T. L. *et al.* 2001. The peroxisome proliferator-activated receptor δ promotes lipid accumulation in human macrophages. *J. Biol. Chem.* **276**, 44 258–44 265.

Westin, S., Kurokawa, R., Nolte, R. T. *et al.* 1998. Interactions controlling the assembly of nuclear-receptor heterodimers and co-activators. *Nature* **395**, 199–202.

Willson, T. M., Lambert, M. H. & Kliewer, S. A. 2001. Peroxisome proliferator-activated receptor γ and metabolic disease. *Annu. Rev. Biochem.* **70**, 341–367.

Wright, H. M., Clish, C. B., Mikami, T. *et al.* 2000. A synthetic antagonist for the peroxisome proliferator-activated receptor γ inhibits adipocyte differentiation. *J. Biol. Chem.* **275**, 1873–1877.

Yamauchi, T., Waki, H., Kamon, J. *et al.* 2001. Inhibition of RXR and PPAR γ ameliorates diet-induced obesity and type 2 diabetes. *J. Clin. Invest* **108**, 1001–1013.

Yasugi, E., Uemura, I., Kumagai, T., Nishikawa, Y., Yasugi, S. & Yuo, A. 2002. Disruption of mitochondria is an early event during dolichyl monophosphate-induced apoptosis in U937 cells. *Zool. Sci.* **19**, 7–13.

Zilberfarb, V., Siquier, K., Strosberg, A. D. & Issad, T. 2001. Effect of dexamethasone on adipocyte differentiation markers and tumour necrosis factor-α expression in human PAZ6 cells. *Diabetologia* **44**, 377–386.

International Journal of
HEMATOLOGY

Identification of Human Neutrophils during Experimentally Induced Inflammation in Mice with Transplanted CD34$^+$ Cells from Human Umbilical Cord Blood

Masaru Doshi, Makoto Koyanagi, Masako Nakahara, Koichi Saeki, Kumiko Saeki, Akira Yuo

Department of Hematology, Research Institute, International Medical Center of Japan, Tokyo, Japan

Received February 10, 2006; received in revised form June 1, 2006; accepted June 22, 2006

Abstract

Nonobese diabetic/severe combined immunodeficiency/γ chain^{null} (NOG) mice are excellent recipients for xenotransplantation and have been especially valuable for the evaluation of human hematopoietic stem cell (HSC) activities. Because human hematopoietic cells that developed in this mouse were mainly lymphoid cells and not myeloid cells, mature human myeloid cells such as neutrophils were hardly detectable in peripheral blood. We demonstrated that human neutrophils accumulated by means of a zymosan-induced air pouch inflammation technique could be identified with a fluorescence-activated cell sorter in NOG mice with transplanted CD34$^+$ cells from human umbilical cord blood, which were putative hematopoietic progenitor cells including HSC. Our results indicate that human neutrophils with a chemotactic capacity can develop from human hematopoietic progenitor cells in vivo, suggesting that our system may be a useful tool for the evaluation of human HSC activities.

Int J Hematol. 2006:84:231-237. doi: 10.1532/IJH97.06040

Key words: NOG mice; Transplantation; Human hematopoietic stem cells; Human neutrophils; Chemotaxis

1. Introduction

Hematopoietic stem cells (HSC) have been defined to possess both the ability to self-renew and the capacity to differentiate into full lineages of hematopoietic cells [1], capabilities that have been evaluated by the transplantation of human cells into experimental animals. Nonobese diabetic/severe combined immunodeficiency (NOD/SCID) mice have widely been used as recipients in xenotransplantation to evaluate the abilities of human HSC, although the engraftment rate of human hematopoietic cells in these mice has been low [2].

NOD/SCID/γ chain (γc)^{null} (NOG) mice, an NOD/SCID mouse strain that lacks the interleukin 2 receptor γc, were recently established to improve the engraftment efficiency of the conventional NOD/SCID mouse, which possesses natural killer cell activity [3]. Several studies have demonstrated that human hematopoietic cells develop in hematopoietic tissue or the peripheral blood of NOG mice that have received transplants of human hematopoietic progenitor cells, such as umbilical cord blood (CB) and bone marrow CD34$^+$ cells containing HSC [3-6]. However, because the human hematopoietic cells that developed in these mice were mainly lymphoid cells and not myeloid cells [4-6], mature human myeloid cells such as neutrophils were hardly detectable in the peripheral blood of the mice that had received such transplants. Therefore, no study has definitely identified human neutrophils in mice with transplanted human hematopoietic progenitor cells.

Human neutrophils, a primary constituent of peripheral blood leukocytes, play an important role during host defense against invading microorganisms [7]. The decreased numbers of neutrophils or attenuated function of neutrophils results in serious infections in several pathologic situations, such as congenital leukocyte function deficiencies or myelosuppression caused by chemotherapy [8,9]. The microbicidal functions of neutrophils are executed via total harmonization of all their specific functions, such as chemotaxis, adhesion, phagocytosis, and respiratory burst activity [10]. Several conventional methods are available to evaluate these effector functions of human neutrophils in vitro [11]. In addition, some functions, such as chemotaxis,

Correspondence and reprint requests: Akira Yuo, MD, PhD, Department of Hematology, Research Institute, International Medical Center of Japan, 1-21-1, Toyama, Shinjuku-ku, Tokyo 162-8655, Japan; 81-3-3202-7181; fax: 81-3-3207-1038 (e-mail: yuoakira@ri.imcj.go.jp).

can be evaluated in vivo by using the acute-inflammation model in mice [12].

Acute inflammation is induced by the injection of zymosan into a dorsal air pouch created in a mouse and the subsequent accumulation of a large number of murine neutrophils into the air pouch [13,14]. Consequently, highly purified murine neutrophils with a sufficient capacity to migrate from other sites, such as the peripheral blood, into inflammatory sites can be isolated from mice by means of this inflammation model. Our objective was to investigate whether the zymosan-injection air pouch methodology can be used in immunodeficient mice with transplanted human HSC to elicit neutrophil migration and inflammation. This methodology gives us the opportunity to evaluate not only human neutrophil production but also critical functions of engrafted human neutrophils.

2. Materials and Methods

2.1. Animals

The experimental protocol was approved by the Committee of Animal Care and Experiments of the Research Institute of the International Medical Center of Japan (IMCJ) (protocol no. 17-Tg-7). NOG mice were purchased from the Central Institute of Experimental Animals (CIEA) (Kanagawa, Japan). All mice were kept under specific pathogen-free conditions at the animal laboratory of the Research Institute of IMCJ in accordance with CIEA guidelines.

2.2. Transplantation of Human CB CD34$^+$ Cells into Mice

Nine-week-old female NOG mice were sublethally irradiated with 2 Gy via an MBR1520-3 x-ray source (Hitachi Medical, Tokyo, Japan). After 24 hours, mice received intravenous transplants of 1.8×10^5 human CB CD34$^+$ cells (AllCells, Berkeley, CA, USA) or vehicle (saline). The purity and viability of the CB CD34$^+$ cells were greater than 95%.

2.3. Zymosan-Induced Air Pouch Inflammation

Six, 8, or 10 weeks after the transplantation of human CB CD34$^+$ cells, a subcutaneous air pouch was formed on the back of NOG mice, as has been described previously [13,14]. Five hundred microliters of zymosan solution (1 mg/mL in saline) was injected into the air pouch. Sixteen hours after zymosan injection, mice were decapitated under diethyl ether anesthesia, and the air pouch was washed with 1 mL of ice-cold phosphate-buffered saline (PBS) to obtain accumulated leukocytes.

2.4. Determination of Superoxide Release

Superoxide release stimulated by phorbol myristate acetate was assayed by the superoxide dismutase–inhibitable reduction of ferricytochrome c, which was monitored continuously in a Hitachi 556 double-wavelength spectrophotometer (Hitachi High-Technologies, Tokyo, Japan) equipped with a thermostatted cuvette holder (37°C), as described previously [11].

2.5. Preparation of Neutrophils from Human Peripheral Blood

Granulocytes and mononuclear cells were prepared from healthy adult donors as described previously [11] by using dextran (Nacalai Tesque, Kyoto, Japan) sedimentation, centrifugation with a separating solution (Lymphoprep; Axis-Shield, Oslo, Norway), and hypotonic lysis of the contaminating erythrocytes. Neutrophils constituted greater than 90% of the granulocyte fractions, and the remaining cells were eosinophils. Mononuclear cell fractions consisted of 20% monocytes and 80% lymphocytes. Both cell fractions were suspended in PBS containing 5% fetal calf serum (FCS).

2.6. Preparation of Murine Bone Marrow and Spleen Leukocytes

Bone marrow cells were harvested from the mice by flushing the femurs with ice-cold Hanks balanced salt solution (HBSS). Spleens were harvested from the mice and minced in ice-cold HBSS. The resulting cell suspensions were filtered through a nylon mesh, and contaminating erythrocytes were eliminated by hypotonic lysis. The cells were then washed once and suspended in PBS containing 5% FCS.

2.7. Determination of Cell Surface Antigens by Fluorescence-Activated Cell Sorting

All suspensions of single cells were stained with the appropriate antibodies and analyzed by fluorescence-activated cell sorting (FACS) with a FACSCalibur flow cytometer (BD Biosciences, San Jose, CA, USA). Cells were incubated with monoclonal antibodies for 30 minutes on ice in PBS containing 5% FCS. Nonspecific binding to cells bearing Fcγ receptors was blocked with a rat antimouse CD16/CD32 monoclonal antibody (BD Biosciences). The following monoclonal antibodies were used in this flow cytometric study: fluorescein isothiocyanate (FITC)-conjugated rat antimouse Ly-6G and Ly-6C antibody (Gr-1 antibody) (BD Biosciences), phycoerythrin (PE)-conjugated mouse antihuman CD45 (BD Biosciences), PE-conjugated mouse antihuman CD10 (BD Biosciences), FITC-conjugated mouse antihuman CD66b (Beckman Coulter, Miami, FL, USA), and each isotype as a control. Antimouse Gr-1 antibody, which reacts selectively with murine neutrophils, does not cross-react with human hematopoietic cells, including neutrophils, and antihuman CD45, CD10, and CD66b antibodies, which react selectively with human neutrophils, do not cross-react with murine neutrophils.

2.8. Immunocytochemical Study

Cells collected from air pouches were washed with PBS and fixed on glass slides by means of a Cytospin apparatus (Cytospin 2; Shandon, Pittsburgh, PA, USA). After further fixation with acetone/methanol solution (1:3), immunostaining was performed as described previously [15] by using FITC-conjugated antihuman CD16b monoclonal antibody (Beckman Coulter) or antihuman CD45 monoclonal

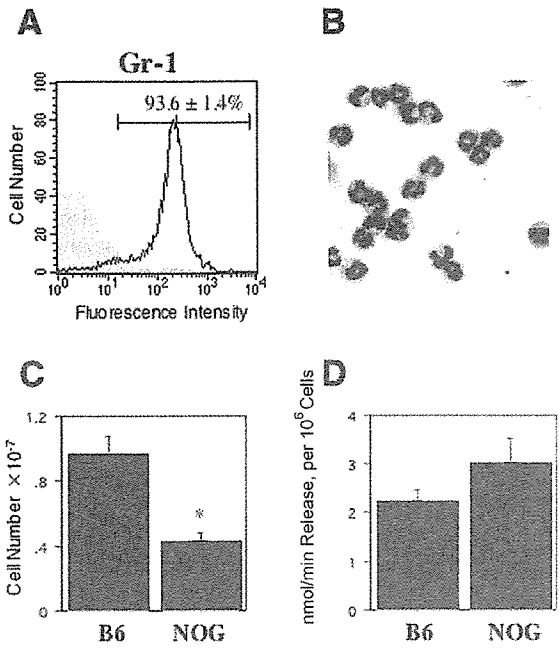

Figure 1. Air pouch inflammatory model in nonobese diabetic/severe combined immunodeficiency/γ chain^{null} (NOG) mice. Zymosan suspended in saline (0.5 mg/mouse) was injected into the air pouch of NOG mice to induce inflammation. The pouch was washed with phosphate-buffered saline 16 hours after zymosan injection to obtain accumulated leukocytes. A, Fluorescence-activated cell-sorting analysis of the expression of the granulocyte-specific antigen Gr-1 was carried out with leukocytes from the air pouch of NOG mice (n = 3). B, Morphology of the leukocytes in the air pouch of NOG mice. After fixation to glass slides, cells were stained with Wright-Giemsa solution and examined by light microscopy. C, The number of leukocytes in the air pouch was determined in B6 and NOG mice. D, The respiratory burst activities of granulocytes in the air pouch in B6 and NOG mice. Superoxide (O_2^-) release stimulated by 100 ng/mL phorbol myristate acetate was determined by the reduction of cytochrome *c* and is expressed as nmol/minute per 10^6 cells. Data for (C) and (D) are expressed as the mean ± SE (n = 6), and statistical analysis was performed by means of an unpaired Student *t* test. **P* < .05, NOG versus B6 mice.

antibody (BD Biosciences). For the control, an isotype antibody reaction was performed by using FITC-conjugated immunoglobulin M (IgM) κ (ICN Biomedicals, Aurora, OH, USA) and IgG1 κ (BD Biosciences) for the anti-CD16b and anti-CD45 antibody reactions, respectively. The second antibody reaction was performed by using Alexa Fluor 488 goat antimouse IgM (Invitrogen, Carlsbad, CA, USA) and Alexa Fluor 488 goat antimouse IgG (Invitrogen) for the anti-CD16b and anti-CD45 antibody reactions, respectively.

2.9. Morphologic Observation

Cells were fixed on glass slides with a Cytospin 2 apparatus, stained with Wright-Giemsa solution (Muto Pure Chemical, Tokyo, Japan), and then observed with a light microscope (Olympus Optical, Tokyo, Japan).

2.10. Statistical Analysis

Statistical analysis was performed by means of the unpaired Student *t* test and the StatView software package (version 5.0; SAS Institute/Abacus Concepts, Berkeley, CA, USA).

3. Results

3.1. Zymosan-Induced Air Pouch Inflammation in NOG Mice

The leukocytes that accumulate by zymosan-induced air pouch inflammation in normal mice are known to be predominantly neutrophils, along with small numbers of monocytes and lymphocytes (data for normal B6 mice are not shown) [13,14]. In the present study, we first investigated whether zymosan-induced accumulation of mature murine neutrophils into the air pouch also occurs in NOG mice.

As has been observed with this inflammatory model in normal mice, the leukocytes that accumulated in the air pouch after zymosan injection in NOG mice were predominantly neutrophils. This result was established by detecting the expression of a specific surface antigen of mouse neutrophils, Gr-1, as well as the typical morphologic characteristics obtained via Wright-Giemsa staining (Figures 1A and 1B). Both the FACS analysis of the Gr-1 antigen and the morphologic evaluation indicated that greater than 90% of the accumulated leukocytes were neutrophils. In the NOG mice lacking lymphocytes, the remaining leukocytes (<10%) were monocytes (data not shown).

These results indicate that the migration of neutrophils toward inflammatory sites occurs almost normally in NOG mice, suggesting that the neutrophils of NOG mice have a normal chemotactic function. The number of leukocytes in the air pouch of NOG mice, however, was significantly lower ($P < .05$) than that of B6 mice (Figure 1C). On the other hand, the respiratory burst activity, another important function of neutrophils, was normal, because agonist-induced superoxide release from the leukocytes in the air pouch of NOG mice was equivalent to that of B6 mice (Figure 1D).

3.2. Engraftment of Human CB CD34⁺ Cells in NOG Mice

We next transplanted human CB CD34⁺ cells into recipient NOG mice. After being sublethally irradiated, NOG mice received intravenous transplants of human CB CD34⁺ cells. Six weeks after transplantation, leukocytes in the bone marrow and spleen were analyzed for the expression of the human panleukocyte marker, CD45 (Figure 2). In these hematopoietic organs, approximately 90% of the cells expressed human CD45 antigen, both at 6 weeks and at 8 weeks after the transplantation of human CB CD34⁺ cells (Figure 2). These findings indicate the highly effective engraftment of human hematopoietic cells in this immunodeficient mouse, and the efficiency of engraftment obtained in

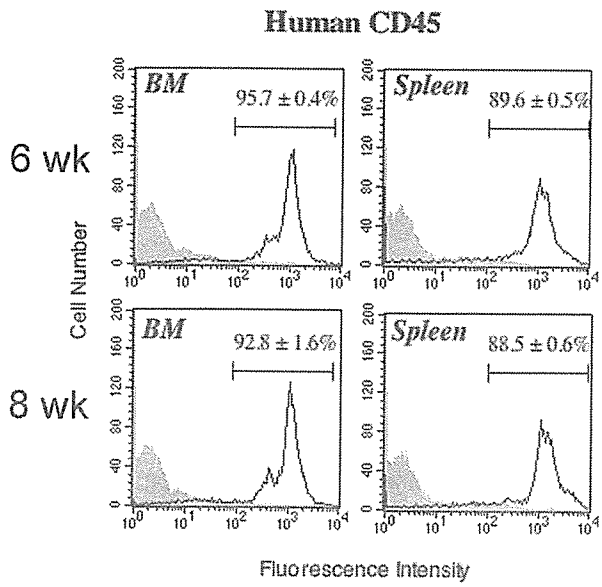

Figure 2. Engraftment of human cord blood CD34⁺ cells in nonobese diabetic/severe combined immunodeficiency/γ chain^{null} (NOG) mice. CD34⁺ cells from human umbilical cord blood (1.8×10^5 cells/mouse) were transplanted into NOG mice intravenously. Bone marrow (BM) and spleen leukocytes were obtained at 6 and 8 weeks after transplantation as described in "Materials and Methods." Cell surface expression of human CD45 was determined by fluorescence-activated cell-sorting analysis. Data are expressed as the mean ± SE (n = 3).

this study was equivalent to or better than the results described in previous reports [3,4].

We then evaluated whether CD45⁺ human hematopoietic cells appear in the air pouch of NOG mice that had received transplants of human CB CD34⁺ cells. As is shown in Figure 3 (upper panel), more than 90% of the leukocytes in the air pouch of NOG mice infused with vehicle alone were Gr-1⁺ murine neutrophils, and there were no human CD45⁺ leukocytes. In contrast, a significant level (approximately 10%) of human CD45⁺ cells in the air pouch was present in NOG mice that had received transplants of human CB CD34⁺ cells, and there was a concomitant decrease in the percentage of Gr-1⁺ murine neutrophils. We observed these findings at both 6 weeks and 8 weeks after transplantation of human CB CD34⁺ cells, although the human CD45⁺ cells in the air pouch had decreased at 8 weeks for an unknown reason.

3.3. Identification of Human Neutrophils Accumulated by Zymosan-Induced Air Pouch Inflammation in Mice with Transplanted Human CB CD34⁺ Cells

Because most of the leukocytes in zymosan-induced air pouch inflammation were neutrophils, the human CD45⁺ leukocytes in Figure 3 were considered human neutrophils that had differentiated in vivo in the NOG mice. To further confirm this hypothesis, we performed FACS analysis with monoclonal antibodies that specifically recognize mature human neutrophils. We selected 2 neutrophil-specific cell surface molecules, CD10 and CD66b. CD10, well known as a common acute lymphoblastic leukemia antigen [16], has been reported to be expressed in mature neutrophils [17-19], and CD66b is a specific cell surface antigen of human granulocytes [20].

Before the transplantation experiments with NOG mice, we performed several experiments with normal human neutrophils and mononuclear leukocytes to establish experimental conditions for the 2-color flow cytometric analysis of CD10 and CD66b. As is shown in Figure 4 (upper panel), we successfully performed 2-color analysis with a granulocyte fraction isolated from a healthy donor. The granulocyte fraction contained 96.5% CD66b⁺ granulocytes, which consisted of 86.3% CD10⁺ neutrophils and 10.2% other CD10⁻ granulocytes, probably eosinophils. This granulocyte fraction contained more than 98% CD45⁺ cells (data not shown). In contrast, the cells in mononuclear cell fractions were negative for both CD66b and CD10.

Using this analytical condition, we then performed a 2-color flow cytometric analysis of the leukocytes that had

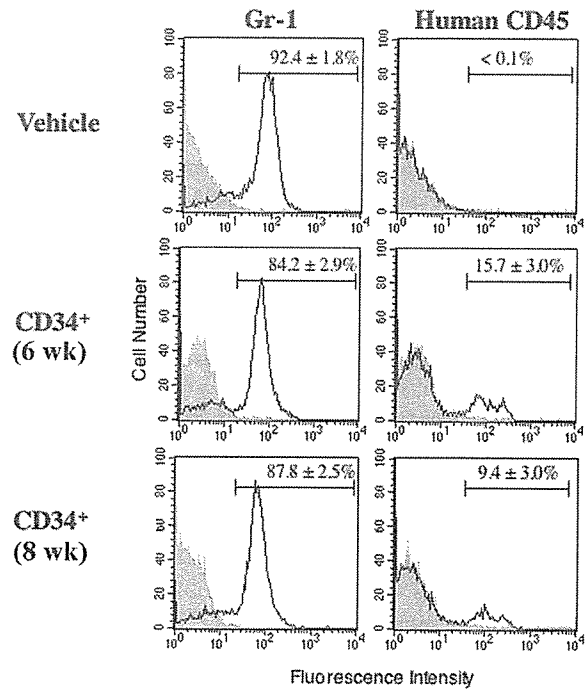

Figure 3. Identification of human leukocytes in the air pouch of nonobese diabetic/severe combined immunodeficiency/γ chain^{null} (NOG) mice. CD34⁺ cells from human umbilical cord blood (1.8×10^5 cells/mouse) (CD34⁺) or saline (vehicle) was transplanted into NOG mice intravenously. Zymosan was suspended in saline (0.5 mg/mouse) and injected into the air pouch to induce inflammation by 6 or 8 weeks after transplantation. The pouch was washed with phosphate-buffered saline 16 hours after zymosan injection to obtain accumulated leukocytes. Cell surface expression of murine Gr-1 and human CD45 was determined by fluorescence-activated cell-sorting analysis. Data are expressed as the mean ± SE (n = 3).

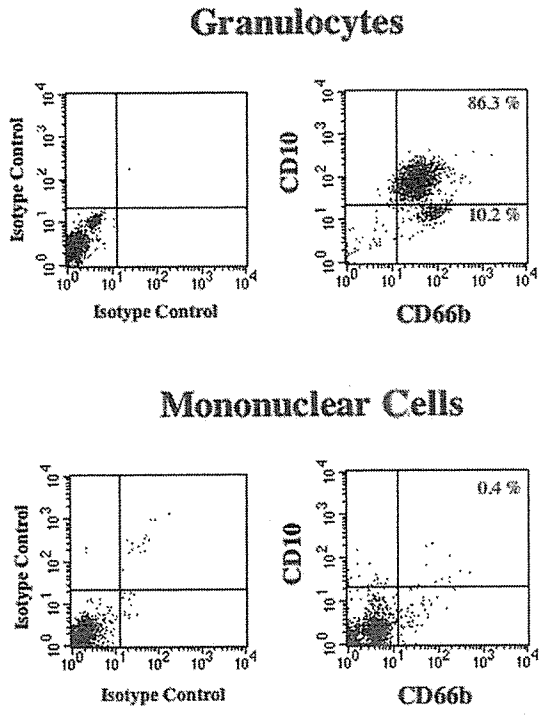

Figure 4. Two-color fluorescence-activated cell-sorting (FACS) analysis of CD10 and CD66b in human peripheral blood leukocytes. Human granulocytes and mononuclear cells were isolated as described in "Materials and Methods." Two-color FACS analysis of the cell surface expression of human CD10 and CD66b was performed with each isotype antibody as a control.

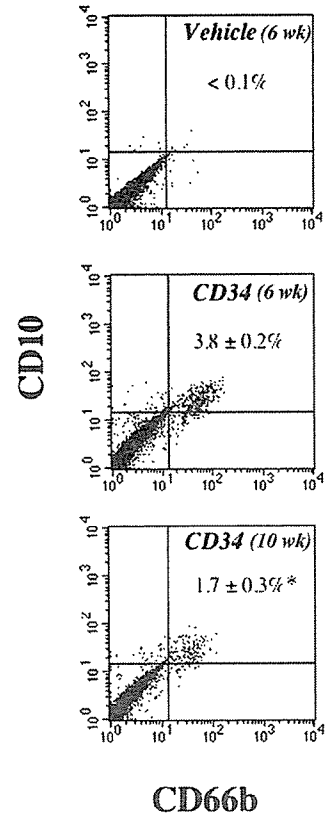

Figure 5. Two-color fluorescence-activated cell-sorting (FACS) analysis of CD10 and CD66b in leukocytes in the zymosan-induced air pouch in nonobese diabetic/severe combined immunodeficiency/γ chain^{null} (NOG) mice with transplanted human umbilical cord blood (CB) CD34$^+$ cells. Human CB CD34$^+$ cells (1.8×10^5 cells/mouse) were transplanted into NOG mice intravenously. Zymosan suspended in saline (0.5 mg/mouse) was injected into the air pouch to induce inflammation at 6 or 10 weeks after transplantation (middle and lower panels). Sixteen hours after zymosan injection, the pouch was washed with phosphate-buffered saline to obtain accumulated leukocytes. Cell surface expression of human CD10 and CD66b was determined by FACS analysis. As a negative control, leukocytes that had accumulated in the air pouch in NOG mice without CD34$^+$ cell transplantation were analyzed, and the results are shown in the top panel. Data are expressed as the mean ± SE (n = 3). Statistical analysis was performed by means of an unpaired Student *t* test. $^*P < .05$, 10 weeks versus 6 weeks.

accumulated in the air pouch after zymosan injection into mice with transplanted human CB CD34$^+$ cells. As is shown in Figure 5, double-positive (both CD10$^+$ and CD66b$^+$) human neutrophils were detected in the air pouch at both 6 weeks and 10 weeks after the transplantation of human CB CD34$^+$ cells. It is interesting that the double-positive human neutrophils in the air pouch had decreased by 10 weeks, compared with the numbers at 6 weeks. These data for double-positive human neutrophils in the air pouch almost corresponded to the data estimated from the numbers of human CD45$^+$ leukocytes in the air pouch (data not shown).

Finally, we used immunocytochemical staining to confirm that human neutrophils actually existed in the air pouch following zymosan injection into mice with transplanted human CB CD34$^+$ cells. As is shown in Figure 6, we were able to detect human CD45$^+$ cells with a neutrophil morphology in the leukocytes that had accumulated in the air pouch of mice with transplanted human CB CD34$^+$ cells. In contrast, human CD45$^+$ cells were not observed in the leukocytes that had accumulated in the air pouch of mice that had not undergone transplantation (data not shown). The presence of human neutrophils in the air pouch of mice with transplanted human CB CD34$^+$ cells was also confirmed with antihuman neutrophil-specific CD16b antibody (Figure 7).

Thus, using an in vivo inflammatory model, we have shown the functional engraftment of human neutrophils.

4. Discussion

Mature human neutrophils derived from human hematopoietic progenitor cells have not been identified in the peripheral blood of immunodeficient mice with transplanted human HSC, although HSC are considered to dif-